GENOMICS, PHOSPHOPROTEOME AND MOLECULAR EPIDEMIOLOGY ANALYSES OF CHLAMYDIA INFECTION

Ph.D. Thesis

Virók Dezső M.D.

Department of Medical Microbiology and Immunobiology
University of Szeged, Faculty of Medicine

Szeged

2007

Contents

Publications with results incorporated in the thesis

I. Virok D, Kis Z, Karai L, Intzedy L, Burian K, Szabo A, Ivanyi B, and Gonczol E: *Chlamydia pneumoniae* in atherosclerotic middle cerebral artery.
Stroke. 2001; 32: 1973-1978. Impact factor: 5,176

II. Virok D, Loboda A, Kari L, Nebozhyn M, Chang C, Nichols C, Endresz V, Gonczol E, Berencsi K, Showe MK, Showe LC.: Infection of U937 monocytic cells with *Chlamydia pneumoniae* induces extensive changes in host cell gene expression.
J Infect Dis. 2003 Nov 1;188(9):1310-21. Impact factor: 4.953

III. Virok DP, Nelson DE, Whitmire WM, Crane DD, Goheen MM, Caldwell HD. Chlamydial infection induces pathobiotype-specific protein tyrosine phosphorylation in epithelial cells.
Infect Immun. 2005 Apr;73(4):1939-46. Impact factor: 3.933

Further publications related to the thesis

I. Burian K, Kis Z, Virok D, Endresz V, Prohaszka Z, Duba J, Berencsi K, Boda K, Horvath L, Romics L, Fust G, Gonczol E.
Independent and joint effects of antibodies to human heat-shock protein 60 and Chlamydia pneumoniae infection in the development of coronary atherosclerosis.
Circulation. 2001 Mar 20;103(11):1503-8. Impact factor: 11.632

II. Virok D, Kis Z, Kari L, Barzo P, Sipka R, Burian K, Nelson DE, Jackel M, Kerenyi T, Bodosi M, Gonczol E, Endresz V.
Chlamydophila pneumoniae and human cytomegalovirus in atherosclerotic carotid plaques--combined presence and possible interactions.
Acta Microbiol Immunol Hung. 2006 Mar;53(1):35-50.

III. Burian K, Berencsi K, Endresz V, Gyulai Z, Valyi-Nagy T, Valyi-Nagy I, Bakay M, Geng Y, Virok D, Kari L, Hajnal-Papp R, Trinchieri G, Gonczol E.
Chlamydia pneumoniae exacerbates aortic inflammatory foci caused by murine cytomegalovirus infection in normocholesterolemic mice.
Clin Diagn Lab Immunol. 2001 Nov;8(6):1263-6. Impact factor: 2.056

Abstracts related to the thesis

I. **Virók D**, Burián K, Endrész V, Korcsik J, Barzó P, Ruzsa Z, Szécsi P, Bodosi M, Gönczöl É: DNA sequences of various herpesviruses and *Chlamydia pneumoniae* in human carotic atherosclerotic plaques. Abstracts of 1st Conference of the Central and Eastern European Stroke Society, Budapest, 1999; p. 20

II. Gönczöl É, Berencsi K, Endrész V, Burián K, Gyulai Zs, Vályi-Nagy T, **Virók D**, Hajnal-Papp R: Atherosclerotic lesions in the aorta after MCMV infection, increased histopathology after dual infection with MCMV and *Chlamydia pneumoniae*. Abstracts of 7th International Cytomegalovirus Workshop, Brighton, UK. J. Clin. Virol. 1999; 12(2):156

III. **Virok D**, Burian K, Endresz V, Korcsik J, Barzo P, Ruzsa Z, Szecsi J, Bodosi M, Gonczol E: Detection of DNA sequences of various herpesviruses and *Chlamydia pneumoniae* in human atherosclerotic plaques. Abstracts of 7th International Cytomegalovirus Workshop, Brighton, UK. J. Clin. Virol. 1999; 12(2):156

IV. Endrész V, Burián K, **Virók D**, Kis Z, Boda K, Prohászka Z, Füst G, Gönczöl É: Human cytomegalovirus and *Chlamydia pneumoniae* specific antibodies in sera of patients with coronary heart disease. Book of Abstracts of 13th Int. Congress of the Hungarian Society for Microbiology, Budapest; 1999; p. 26-26

V. Burián K, Berencsi K, Endrész V, Gyulai Zs, Vályi-Nagy T, **Virók D**, Hajnal-Papp R, Gönczöl É: Inflammation and advanced atherosclerotic lesions after MCMV infection, increased histopatology after consecutive infection with MCMV and *Chlamydia pneumoniae*. 3rd Annual Meeting of ESCV, Progress in Clinical Virology V., Budapest, Acta Microbiol. Immunol. Hung. 1999; **46**, 379-380

VI. **Virók D**, Barzó P, Ruzsa Z, Burián K, Endrész V, Szécsi P, Bodosi M, Gönczöl É: *Chlamydia pneumoniae* and various herpesvirus DNA in human atherosclerotic plaques. Magyar Mikrobiológiai Társaság Nagygyűlése, Acta Microbiol. Immunol. Hung. 1999; **46**, 470-471

VII. Kis Z, **Virók D**, Endrész V, Burián K, Iványi B, Vécsei L, Gönczöl É: *Chlamydia pneumoniae* DNS jelenléte agyi erekben valamint stroke-ban szenvedő betegek és egészséges véradók perifériás vér mononukleáris sejtjeiben. Magyar Mikrobiológiai Társaság Nagygyűlése, Balatonfüred, 2001. évi Jubileumi Nagygyűlés előadásainak összefoglalója: p. 81.

Abbreviations

AT	atherosclerosis
C. caviae	*Chlamydophila caviae*
C. muridarum	*Chlamydia muridarum*
C. pneumoniae	*Chlamydophila pneumoniae*
C. trachomatis	*Chlamydia trachomatis*
C.psittaci	*Chlamydophila psittaci*
CSF	colony stimulating factor
EB	elementary body
ECM	extracellular matrix
ET	endothelin
FABP	fatty acid binding protein
FBS	fetal bovine serum
FGF	fibroblast growth factor
GAG	glucoseaminoglycane
GPIC	guinea pig inclusion conjunctivitis
GRO	growth related oncogene
HBEGF	heparin binding epithelial growth factor
hsp	heat shock protein
IFU	infectious unit
IKB	inhibitor of nuclear factor - kappa beta
kDa	kilodalton
LGV	lymphogranuloma venereum
MCP	monocyte chemotactic protein
MIP	macrophage inflammatory protein
MMP	matrix metalloproteinase
MOI	multiplicity of infection
MOMP	major outer membrane protein
NFKB	nuclear factor - kappa beta
nMD	normalized median density
nPCR	nested PCR
p.i	post infection
PBMC	peripherial blood mononuclear cell
PDGF	platelet derived growth factor
pmp	polymorphic membrane protein
PPBP	pro-platelet basic protein
RB	reticulate body
TEM	transmission electron microscopy
TNF	tumor necrosis factor

1. Summary

Chlamydophila pneumoniae (*C. pneumoniae)* is an obligate intracellular bacterium primarily associated with respiratory infections, including pneumonia and bronchitis. It is widely distributed in the population, and by age 20, ~50% of the population of the developed world is seropositive (Grayston 2000). Infection with the bacterium has been suggested to contribute to the initiation and/or progression of a variety of chronic inflammatory diseases, including multiple sclerosis (Yucesan and Sriram 2001), asthma (Esposito and Principi 2001) and atherosclerosis (Campbell, Kuo et al. 1998). Atherosclerotic middle cerebral arteries are frequent sites of thrombosis, leading to stroke. However, the presence of this pathogen in atherosclerotic middle cerebral arteries has not been documented. We analyzed atheromatous plaques from middle cerebral arteries for the presence of *C. pneumoniae*. Atherosclerotic middle cerebral arteries from 15 cadavers who died of natural causes and corresponding nonatherosclerotic arteries from 4 otherwise healthy trauma victims were examined. Assays for *C. pneumoniae* DNA were carried out by nested polymerase chain reaction (nPCR) specific for the *C. pneumoniae* ompA gene. The presence of the bacterium was assessed by transmission electron microscopy. Five of the 15 atherosclerotic arterial samples and none of the control tissues were positive for *C. pneumoniae* by nPCR. Particles similar in morphology and size to *C. pneumoniae* elementary bodies were detected by transmission electron microscopy in 4 of the 5 nPCR-positive atherosclerotic samples. The demonstration of *C. pneumoniae* in atherosclerotic middle cerebral arteries is consistent with the hypothesis that this bacterium is involved in acute and chronic cerebrovascular diseases.

Human moncytes and monocyte derived macrophages are important cells for both the spreading of *C. pneumoniae*, and the development of atherosclerosis. We studied the effect of infection with *C. pneumoniae* on host messenger RNA expression in human monocytic cells with DNA microarrays. The data chronicle a cascade of transcriptional events affecting 128 genes, many of which have not previously been reported to be affected by *C. pneumoniae* infection. Downregulated genes are primarily associated with RNA and DNA metabolism, chromosomal stability, and cell-cycle regulation. Upregulated mRNAs include those for a variety of genes with important proinflammatory functions such as

monocyte chemotactic protein-1 (MCP-1), MCP-2, macrophage inflammatory protein-1alpha (MIP-1α), MIP-1β, MIP2-β, interleukin-1beta (IL-1β) and matrix metalloproteinase-3 (MMP-3), MMP-10, MMP-12. We showed novel *C. pneumoniae* induced host cell genes —including the hyaluron receptor CD-44, vasoconstrictor endothelin-1, the smooth muscle growth factor heparin-binding EGF-like growth factor, pro-platelet binding protein and fatty acid binding protein–4, coagulation factor-V—that had not been connected to *C. pneumoniae* monocyte infection before, but had been previously described as characteristics for the development of atherosclerosis and other chronic inflammatory diseases. We concluded that *C. pneumoniae*–infected monocytes can contribute to the development and progression of diseases for which acute or chronic inflammation has been shown to be important, such as atherosclerosis.

Members of the genus *Chlamydia* exhibit marked differences in host range and tissue tropism despite sharing a remarkable level of genomic synteny. These pathobiotype differences among chlamydiae are also mirrored in their early interactions with cultured mammalian host cells. Chlamydial attachment and entry is known to trigger protein tyrosine phosphorylation. We examined the kinetics and pattern of protein tyrosine phosphorylation induced by infection with a comprehensive collection of chlamydial strains exhibiting diversity in host, tissue, and disease tropisms. We reported new findings showing that protein tyrosine phosphorylation patterns induced by infection directly correlated with the pathobiotype of the infecting organism. Patterns of protein tyrosine phosphorylation were induced following early infection that unambiguously categorized chlamydial pathobiotypes into four distinct groups: (i) *C. trachomatis* trachoma biovars (serovars A to H), (ii) *C. trachomatis* lymphogranuloma venereum biovars (serovars L_1 to L_3), (iii) *C. muridarum*, and (iv) *C. pneumoniae* and *C. caviae*. Notably, chlamydia infected murine and human epithelial cells exhibited the same protein tyrosine phosphorylation patterns; this is indirect evidence suggesting that the phosphorylated protein(s) is of chlamydial origin. If our hypothesis is correct, these heretofore-uncharacterized proteins may represent a novel class of bacterial molecules that influence pathogen-host range or tissue tropism.

2. *Introduction*

Chlamydia genus contains obligate intracellular bacteria that are characterized by a unique biphasic life cycle. Infection starts with the attachment of the infectious, metabolically non-active form of the bacterium, the elementary body (EB) to the host cell cytoplasm. The EB induces a host cytoskeletal rearrangement and phagocytosed or endocytosed into the host cytoplasm. The bacterium evades the fusion of the lysosomes by an unknown mechanism, and relocates to the perinuclear space using the host microtubular network. The EB rapidly differentiates into the metabolically active form of the bacterium, the reticulate body (RB). The RB undergoes multiple rounds of binary fission, in a protected niche called inclusion. The RB then transforms to EB and the infectious EBs are released from the host cell.

The main commonly studied strains of chlamydia are *C. trachomatis*, *C. muridarum*, *C. pneumoniae and C.caviae*. *C. trachomatis* multiplicates in the epithelial cells of the oculo-urogenital system and consist of 15 major serovariants grouped into two biovars the trachoma biovar (serovars A-K) and LGV biovar (serovars L_1-L_2-L_3). Serovars A, B, Ba and C cause trachoma, an inflammation of the keratoconjunctiva that can lead to extensive scarring and eventually blindness. Serovars D-K cause local inflamation of the urogenital system such as urethritis, cervicitis, endometritis, salpingitis. These pelvic inflammations also can lead to scarring, resulting tubal occlusion and ectopic pregnancy or infertility. Serovars L_1-L_2-L_3 cause lymphogranuloma venereum, a disseminated infection of the urogenital system and the surrounding lymph nodes. *C. trachomatis* infection has great medical importance, this is the most common sexually transmited disease in the world, and the leading cause of preventable blindness (Thylefors 1995; WHO 1996). The mouse strain of *C. trachomatis* is now called *C. muridarum*. This bacterium causes inflammation of the keratoconjunctiva, the urogenital system and the lung in mice. This strain is important, because the murine model is the most widely used animal model to mimic human infection and for vaccine development. The other medically important human pathogen strain is the *C. pneumoniae,* that causes inflammation of the respiratory tract, and is suspected to be involved in a variety of chronic diseases, including multiple sclerosis (Yucesan and Sriram 2001), asthma (Esposito and Principi 2001), Sezary syndrome (Abrams, Balin et al. 2001), and atherosclerosis (Campbell, Kuo et al. 1998).

C. caviae includes strains formerly belonging to *C.psittaci* guinea-pig inclusion conjunctivitis (GPIC) - a genetically close relative of *C. pneumoniae*. The primary target tissue of the bacterium is the mucosal epithelium of guinea pigs resulting conjunctivitis and genital tract infections.

Despite the fact that the genome, the morphology, the unique biphasic developmental cycle are similar between the chlamydia strains, there are also significant differences in the dynamics of chlamydia infections not just *in vivo* but *in vitro*. The *C. trachomatis* trachoma biovars and *C. pneumoniae* require centrifugation for efficient infection, and the trachoma biovars also requires DEAE-dextrane. There are additional differences: inhibition of the host cell`s protein synthesis by cycloheximide increases the growth of *C. trachomatis* trachoma biovars and *C. pneumoniae,* while others don`t require this treatment. The growth rate also varies between the strains: the *C. trachomatis* LGV biovars, *C. muridarum* and *C.psittaci* strains have short developmental cycle (24-36h), while *C. trachomatis* trachoma biovars and *C. pneumoniae* develop slowly in the host cells (~48h).

What is the source of these in vivo and in vitro differences between strains related to the same *Chlamydia* genus? The whole genome sequences of at least five chlamydial strains are available now (http://cmr.tigr.org/tigr-scripts/CMR/CmrHomePage.cgi). The differences at the genome level may help to explain the in vivo and in vitro phenotypic differences. One of the milestone papers in this field is the *C. pneumoniae* and *C. trachomatis* comparative genomics paper (Kalman, Mitchell et al. 1999). Analysis of the 1,042,519 nucleotide length *C. trachomatis* genome and the 1,230,230 nucleotide length *C. pneumoniae* genome revealed that there were 894 and 1073 likely protein coding genes in the two genomes respectively. The fact that the two genus has a similar developmental cycle in the host cell, suggests that there is a high level of functional conservation between the two genomes. There are 859 protein coding genes in the *C. pneumoniae* genome that has orthologues to *C. trachomatis* genes. In addition to these core genes, there are 70 unique *C. trachomatis* genes and 214 genes unique to *C. pneumoniae* likely responsible for the differences in the in vivo virulence and in vitro growth. The detailed analysis of these genome differences is beyond the scope of this thesis, but it is noteworthy that the major part of the increased genome size of *C. pneumoniae* is due to the expansion of the

chlamydial polymorphic membrane protein family (pmp). Many of these genes were found to be on the chlamydial surface, and probably they are involved in the species-specific attachment and/ or entry (Christiansen, Pedersen et al. 2000).

During the entry, the EB binds to heparin or heparane sulphate glucosaminoglycane attached host cell receptor, probably via its abundant cell surface molecule, the major outer membrane protein (MOMP) (Su, Raymond et al. 1996) and/or the heparin and heparane-sulphate molecules that also can be found on the surface of the EBs and host cells (Zhang and Stephens 1992). The attachment is followed by an actin-cytoskeleton reorganization, and entry into the target cells (Carabeo, Grieshaber et al. 2002). The differences in attachment and the subsequent entry and entry-mediated signal-transduction can contribute to the observed in vivo host and tissue tropism. Indeed, *C. pneumoniae* uses the mannose 6-phosphate/ insulin-like growth factor receptor for infection of human endotelial cells, while the *C. trachomatis* E and L_2 probably uses another host cell receptor for attachment and entry (Puolakkainen, Kuo et al. 2005). There are differences in the subsequent chlamydia mediated host signal-transduction as well. *C. trachomatis* did not require the small Rho-GTPase cdc42 for actin polymerization during entry, while the entry of *C. caviae* GPIC needs cdc42 (Subtil, Wyplosz et al. 2004).

The receptor tyrosine kinase and other tyrosine kinase mediated tyrosine phosphorylation is an important part of the signal transduction cascade. There are several examples in other bacterial systems, that the bacterial attachment/entry processes is accompanied by the tyrosine phosphorylation of different groups of bacterial and host proteins. Enteropathogenic *Escherichia coli* (EPEC) bacterium uses a type III. secretion system to deliver its effector protein Tir into the host epithelial cell, where the translocated protein becomes tyrosine phosphorylated (TirPY) (Kenny, DeVinney et al. 1997). The translocated Tir serves as a receptor for the bacterium's own ligand, the intimin protein. Interesingly, the tyrosine phosphorylation is not a requirement for the Tir-intimin binding, however the subsequent host actin-polymerisation and pedestal formation is dependent on the phopsphorylated Tir (Hawrani, Dempsey et al. 2003). Virulent *Helicobacter pylori* strains carry a cag pathogenicity island containing a type IV. secretion system. One of the secreted bacterial effector proteins, CagA becomes tyrosine phosphorylated in the target cell and induces a global actin-cytoskeleton reorganization with a cell elongation

phenotype (Segal, Cha et al. 1999). The phosphorylation of the CagA Y972 is required for the host cell elongation (Backert, Moese et al. 2001).

The availability of anti-phosphotyrosine antibodies made it possible to study the global tyrosine phosphorylation in response to a bacterial infection (Rosenshine, Donnenberg et al. 1992; Pace, Hayman et al. 1993; Segal, Falkow et al. 1996). The complex tyrosine phosphorylation pattern induced by chlamydia infection was also studied previously using pan-phosphotyrosine antibody (Birkelund, Johnsen et al. 1994; Fawaz, van Ooij et al. 1997; Stephens, Fawaz et al. 2000; Clifton, Fields et al. 2004). For *Chlamydia*, Birkelund et al. (Birkelund, Johnsen et al. 1994) described first that the *C. trachomatis* serovar L_2 is capable to induce the tyrosine-phosphorylation of at least three groups of proteins, a ~64, 66, 68 kD triple band, a 97 kD and a 140 kD bands in HeLa human epithelial cells. Fawaz et al. also infected HeLa cells with *C. trachomatis* serovar L_2 and observed a tyrosine-phosphorylation in the 75kD region and the 100kD region reproducibly and several high molecular weight bands occasionally. Chloramphenicol and rifampycin pretreatment of the host cell did not influence the *C. trachomatis* serovar L_2 induced tyrosine phosphorylation. The protein phosphorylation was independent from either the host or chlamydial *de novo* protein synthesis (Fawaz, van Ooij et al. 1997). The induced tyrosine-phosphorylation was MOI dependent: it could not be observed when MOI of 16 or less was used. The above described 64, 66, 68 kD triple band appeared at MOI of 32, and a 97 kD and a 140 kD phosphoprotein appeared when MOI of >100 was used. The tyrosine phosphorylation of the 68-, 66-, and 64-kD triple bands could be detected as early as 15 min after infection of HeLa cells with *C. trachomatis* serovar L_2. The intensity of the triple band reached maximum at 2 to 4 h postinfection and remained detectable as late as 16 hours post infection (Birkelund, Johnsen et al. 1994). The same time-course of tyrosine phosphorylation was observed by others (Fawaz, van Ooij et al. 1997) (Clifton, Fields et al. 2004).

The tyrosine phosphorylation was adjacent to the chlamydia EB as soon as 30 second post infection (Clifton, Fields et al. 2004). The tyrosine phosphorylated protein was located at the periphery of the cells two hours post infection. Similar to the movement of the chlamydial EB itself, the tyrosine phosphorylated protein was migrated towards the perinuclear region of the host cells at four hours post infection. Eighteen hours post

infection, when the EBs transformed to RBs and localized to the perinuclear region, the tyrosine phosphorylated proteins were seen as aggregates at the same region. Double labeling experiments showed that the tyrosine phosphorylated circular structures were identical to the chlamydial inclusions (Birkelund, Johnsen et al. 1994). Fawaz et al. also observed similar pattern of tyrosine phosphorylation and chlamydia immunoreactivity (Fawaz, van Ooij et al. 1997).

The chlamydia induced specific tyrosine-phosphorylation pattern was also observed in different mouse cell types, such as the mouse fibroblast cell line L929, the mouse monocyte-macrophage cell line RAW and the mouse macrophage-like cell line J774.1 leading to the conclusion that the tyrosine-phosphorylation was not host cell species and cell-type specific. It is interesting that the observed tyrosine-phosphorylation pattern in the case of *C. trachomatis* serovar L_2 were similar to the one described previously (Birkelund, Johnsen et al. 1994), however there was a significant size difference in the ~70 kD region between *C. trachomatis* L_2 (~75 kD) and *C. muridarum* induced tyrosine phosphorylation (~85 kD) (Fawaz, van Ooij et al. 1997). The fact, that these phenotypically distinct strains, the mouse mucosal strain *C. muridarum* and the human, non-mucosal, disseminating strain *C. trachomatis* serovar L_2 induced different tyrosine phosphorylation in the target cells, suggests that may be one of the distinguishing features between the biologically different but genotipically sometimes remarkably similar chlamydial strains is the way of entry, and particularly the pattern of the induced tyrosine-phosphorylated proteins.

Amongst the chlamydial strains significant evidences have been accumulated between *C. pneumoniae* infection and systemic chronic inflammatory diseases, particularly atherosclerosis. One of the most current theory of atherosclerosis is the response to injury model. This model includes an endothelial malfunction or activation as a first step of the process. There are multiple traditional risk factors that can activate the endothelial layer such as cigarette smoking, hyperlipidaemia, hyperglycaemia, turbulent blood flow, circulating immune complexes. This activation leads to increased expression of certain receptors such as E-selectin, P-selectin, ICAM-1, VCAM-1 on the surface of the endothelial cells. The blood monocytes start to roll and adhere to the activated endothelial cell layer using their endothelial receptor ligands E-selectin ligand-1, P-selectin glycoprotein ligand-1 and β1- and β2-integrins. After the attachment to the endothelium,

the blood monocytes transmigrate to the subendothelial space following a local MCP-1 (monocyte chemotactic protein-1) and IL-8 chemokine gradient and differentiate to macrophage by the local monocyte colony stimulating factor (M-CSF) and granulocyte-monocyte colony stimulating factor (GM-CSF). The macrophages express scavenger receptors SRA and CD-36, and accumulate a large amount of lipids in their cytoplasm. These lipid-laden macrophages are characteristic features of the early atherosclerotic lesion. This early plaque could develop further to the so-called complicated plaque. This development is characterized by a dynamic balance of tissue development and destruction in the vessel wall. The local macrophages start to express different matrix metalloproteinases destructing the surrounding extracellular matrix, and endothelial basal membranes. This process leads to plaque rupture, and the development of surface or intramural thrombus. The aggregated thrombocytes secrete platelet derived growth factor (PDGF), a potent mitogen of the local smooth muscle cells and fibroblasts and in accordance with other local mitogens such as basic and acidic fibroblast growth factor (FGF) enhance the proliferation of fibroblasts and smooth muscle cells and extracellular matrix production. This tissue growth and thrombus formation together significantly decrease the diameter of the vessel wall leading to clinical signs suchs acute myocardial infarct or stroke (for a review of atherosclerosis development see (Libby 2002)).

In addition to the traditional risk factors, the role of certain infections in the initial endothelial injury was proposed almost 120 years ago (Gilbert A). More than twenty different pathogens have been studied, but the strongest link was found between *C. pneumoniae* infection and atherosclerosis. The first study that found an elevated anti-chlamydia titer in patients with coronary atherosclerosis compared to healthy controls was published by Saikku et al. in 1988 (Saikku, Leinonen et al. 1988).

After this groundbreaking study, many follow-up studies showed a significant correlation between *C. pneumoniae* infection and atherosclerosis (Grayston 2000), however in most of the cases seropositivity only moderately increased the risk of atherosclerosis. Combination of *C. pneumoniae* seropositivity with other markers of inflammation, such as increased level of CRP, or other risk factors, such as smoking, can increase the risk significantly. Burian et al. showed that if the atherosclerotic patient group was divided into subgroups based on e.g. the anti-human hsp60 titer, than the chlamydia

and human hsp60 seropositivity together had increased the risk of atherosclerosis 82 fold (Burian, Kis et al. 2001). This important study suggests that chlamydia infection acts together with other traditional risk factors in the development of atherosclerosis.

Immunohistochemistry, electron microscopy, in situ hybridization, PCR and RT-PCR (Grayston 2000) studies also showed the presence of the pathogen's DNA and/ or protein in atherosclerotic tissues of various parts of the vascular system but not or rarely from normal vessels. It is interesting that while one of the major consequences of late atherosclerosis is the stroke, the presence of *C. pneumoniae* in intracerebral arteries has not been well investigated. Case-control studies revealed that specific anti-*C. pneumoniae* antibody levels were significantly higher in patients with cerebrovascular disease than in control patients, (Wimmer, Sandmann-Strupp et al. 1996; Cook, Honeybourne et al. 1998; Elkind, Lin et al. 2000) and a follow-up study indicated that high antibody titers to *C. pneumoniae* were associated with an increased risk of future stroke (Fagerberg, Gnarpe et al. 1999). Immunoreactivity to *C. pneumoniae*-specific antigen was demonstrated in a low percentage of anterior and posterior cerebral arteries but not in middle cerebral arteries (Vink, Poppen et al. 2001). In addition to seroepidemiology and molecular epidemiology several animal model experiments and antibiotic trials, although not uniformly also showed a link between *C. pneumoniae* infection and atherosclerosis (Moazed, Kuo et al. 1996; Moazed, Kuo et al. 1997) (Moazed, Campbell et al. 1999; Blessing, Lin et al. 2000; Campbell, Rosenfeld et al. 2000; Sander, Winbeck et al. 2002; Higgins 2003; Sander, Winbeck et al. 2004).

Despite the fact that *C. pneumoniae* has been detected at various sites of the vascular tree, the exact mechanism of the spreading from the site of the primary infection, the lung epithelial layer to different tissues, e.g the vessel wall is not known. The current model proposes a *C. pneumoniae* transfer from the infected lung epithelial cells to the local alveolar macrophages, and these cells serve as a vector to disseminate in the body. In a mouse chlamydia model it was showed that *i,* 3 days after intranasal infection *C. pneumoniae* was detected in alveolar macrophages by culture and PCR *ii,* the transfer of infected alveolar macrophages to healthy mice lead to a systemic spreading. The pathogen was detected in the lung, spleen and abdominal lymph nodes of the recipient animal (Moazed, Kuo et al. 1998). However *C. pneumoniae* is not just using the monocytes-

macrophages as a vector, but stimulate these cells, activate them to roll and adhere to the endothelial layer of the vessel wall, transmigrate to the subendothelial space and to initiate and/ or boost the local inflammation. *C. pneumoniae* infected fluorescently labeled mouse macrophages showed a 3-fold increase of rolling and 2-fold adherence to the carotid arteries compared to noninfected macrophages. The endothelial receptor ligands VLA-4, LFA-1, Mac-1 are upregulated in the infected macrophages (May, Redecke et al. 2003), and also these cells secrete a variety of proinflammatory proteins such as MCP-1, IL-8, TNF-α (Kothe, Dalhoff et al. 2000), MMP-1, MMP-9 (Kim, Gaydos et al. 2005), tissue factor (Bea, Puolakkainen et al. 2003) that are important part of the atherosclerosis pathology. The development of atherosclerosis is a long-term process, and from this viewpoint it is noteworthy that while *C. pneumoniae* is able to survive inside the monocytes and macrophages for several days (Kaul and Wenman 2001) *i,* macrophages can transmit locally the infection to more susceptible cell lines such as endothelial cells (Lin, Campbell et al. 2000) and therefore maintain viable locally for a longer period of time *ii,* after the descruction of the bacterium, acellular components of the chlamydia also can enhance local inflammation. Acellular, non-LPS components of the chlamydial vessel wall were able to induce MCP-1, IL-1β, IL-6, IL-8, MIP-1α (macrophage inflammatory protein–1α), TNF-α in PBMCs in a TLR-2 dependent manner (Netea, Selzman et al. 2000; Netea, Kullberg et al. 2002). Chlamydial outer membrane proteins omp2, and the major outer membrane protein (MOMP) and hsp-60 induced a 92 kDa gelatinase production in human monocyte derived macrophages (Vehmaan-Kreula, Puolakkainen et al. 2001). Moreover chlamydial LPS can induce the uptake of cholesteryl-ester and foam-cell formation in the murine macrophage cell line RAW 264.7 (Kalayoglu and Byrne 1998).

It is also noteworthy that *C. pneumoniae* can interact with other potentially proatherosclerotic pathogens such as human cytomegalovirus to costimulate monocytes. We showed that *C.pneumoniae* and human cytomegalovirus coinfected human monocytoid cells produced significantly more proatherosclerotic genes, such as pro platelet basic protein and fatty acid binding protein-4 mRNA, than the singly infected or noninfected control (Virok, Kis et al. 2006). The same phenomena could also be observed *in vivo*. The early atherosclerotic foci induced by murine cytomegalovirus infection were significantly

exacerbated following a single inoculation with *C. pneumoniae* (Burian, Berencsi et al. 2001).

I started my PhD. studies at 1997 to investigate the link between atherosclerosis and *C. pneumoniae*. *C. pneumoniae* was detected from various sites of the vascular system, but the presence of *C. pneumoniae's* DNA in some pathologically important regions, such as in middle cerebral arteries was not studied earlier, despite the fact that these arteries are frequent sites of thrombosis leading to stroke. Moreover, while monocytes are essential for *both* the dissemination of *C. pneumoniae* in the body, and the pathogenesis of atherosclerosis there was no large-scale dataset available about the impact of *C. pneumoniae* on the gene expression of monocytes. Finally, I extended my work to study the chlamydia induced early tyrosine-phosphorylation patterns that distinguish between the different chlamydial strains during the early interaction with the host cell, the attachment and entry processes.

2.2. Aims

The present study was designated to address the following aims:

Aim 1. To determine the presence of *C. pneumoniae* in atherosclerotic and normal human middle cerebral arteries.

Aim 2. To obtain a detailed description of *C. pneumoniae* infection on the gene expression of human monocytes using the high-throughput DNA-chip method.

Aim 3. To determine whether there are differences between the major chlamydial strains during the early interaction of the host cell, particularly comparing the chlamydia-induced early tyrosine-phosphorylation cascade.

3. Materials and Methods

3.1. Study population for the identification of C. pneumoniae in atherosclerotic middle cerebral arteries

Atherosclerotic samples of middle cerebral arteries were obtained from 15 consecutively autopsied subjects. Samples were collected within 24 hours after death with the use of sterile instruments. Half of each sample was frozen at -70°C for nested PCR (nPCR) analysis; the other half was fixed in 3% glutaraldehyde for TEM and histology. For control tissues, samples of 4 nonatherosclerotic middle cerebral arteries were collected from trauma victims who died (at ages 31 to 40) during the study period. Histological assessment of the vessel samples from the 15 patients indicated moderate or severe atherosclerotic stenosis. The control samples from the trauma victims were assessed as histologically normal. The study was approved by an institutional review committee.

3.2. DNA extraction, C. pneumoniae specific nested PCR and transmission electron microscopy

DNA was extracted rom frozen samples with the High Pure PCR Template Preparation Kit (Boehringer-Roche) according to the manufacturer's instructions. Samples from cases or controls were tested in a blinded fashion for *C. pneumoniae* DNA with a GeneApm 2400 PCR system (Perkin-Elmer) with the use of nPCR primer pairs specific for the *C. pneumoniae* ompA gene (Tong and Sillis 1993) resulting in a 206-bp nPCR fragment. The presence of intact DNA was tested for each sample with the use of primers specific for the human ß-actin gene. DNA extracted from the lysate of *C. pneumoniae*-infected McCoy cells (both from American Type Culture Collection) was used as a positive control. The negative control was sterile distilled water subjected to the same extraction procedure as used for the tissue samples. For every set of 5 tested samples, nPCR including the negative control template was carried out. Strict precautions were taken to avoid contamination during DNA extraction and the preparation of the reaction mixture. Problems and limitations of PCR were considered as suggested (Fredricks and Relman 1999; Pfaller

2001) . DNA samples amplified by the *C. pneumoniae* primers were sequenced with the ABI Prism DNA Sequencing Ready Detection Kit (Perkin-Elmer). Fixed samples of the 5 *C. pneumoniae* nPCR-positive arteries and also the 5 *C. pneumoniae* nPCR-negative samples were postfixed in OsO_4 and embedded in Epon. Thin sections stained with uranyl acetate and lead citrate were examined by TEM. McCoy cells infected with *C. pneumoniae* were treated similarly for morphological comparison.

3.3 C. pneumoniae propagation and inoculum preparation for U937 human monocytic cell line infection.

C. pneumoniae (AR-39 strain; obtained from ATCC) was propagated in McCoy cells (ATCC CRL-1696), in MEM with Earle salts supplemented with 10% heat-inactivated fetal bovine serum (FBS), 0.5% glucose, 2 mmol/L L-glutamine, 1× nonessential amino acids (Sigma), 8 mmol/L HEPES, 25 μg/mL gentamycin, and 1 μg/mL cycloheximide. Infected cells were harvested on day 3 or 4 and then disrupted by 2 cycles of freeze-thawing and ultrasonication. Cell debris was removed by centrifugation at 300 *g* for 10 min, and bacteria were concentrated by centrifugation at 30,000 *g* for 30 min. Pellets were resuspended in PBS (pH 7.4), mixed with an equal volume of sucrose-phosphate-glutamic acid buffer (0.22 mol/L sucrose, 10 mmol/L NaH_2PO_4, 3.8 mmol/L KH_2PO_4, and 5 mmol/L glutamic acid [pH 7.4]), formed into aliquots, and frozen at -80°C until use. The same stock was used for all experiments. For mock infection, uninfected McCoy cells were processed as described above and stored at -80°C. *C. pneumoniae* titration was performed on McCoy cells by use of immunofluorescent staining. Monolayers were infected with serial dilutions of concentrated bacteria, incubated for 48 h, fixed with methanol/acetone (1 : 1), and stained with mouse anti–*C. pneumoniae* MOMP monoclonal antibody (Dako). Fluorescein isothiocyanate (FITC)–labeled anti–mouse IgG (goat $F[ab']_2$ anti–mouse IgG; Sigma) was used as a secondary antibody. After counting chlamydial inclusions under a fluorescent microscope, titers were expressed as inclusion-forming units per milliliter.

3.4 U937 human monocytic cell line culture and infection

U937 cells were grown in 75-cm^2 culture flasks in RPMI 1640 medium containing 10% heat-inactivated FBS and 50 μg/mL gentamycin at 37°C in 5% CO_2. Before infection, the

cells were transferred to 24-well plates at a density of 1×10^6 cells/well in RPMI 1640 medium containing 10% heat-inactivated FBS, 0.5% glucose, and 10 mmol/L HEPES. U937 cells were infected with mycoplasma-free *C. pneumoniae* strain AR-39 stock at a multiplicity of 4 IFU/cell. Control cells were treated with the same volume of mock stock. Both were centrifuged at 600 *g* for 45 min at 30°C, during which time infection took place (Kuo and Grayston 1990). The plates were incubated at 37°C and 5% CO_2, and infected and mock-infected cells were collected for RNA extraction at 0, 2, 6, 10, 24, and 48 h after the centrifugation. Note that the zero time point is taken immediately after the 45-min centrifugation of the bacteria, during which time infection occurs. Cells were washed twice with 37°C medium used for infection before extracting the RNA. Three independent experiments monitored by cDNA arrays were performed. Two additional experiments with the same conditions were performed, to compare the *C. pneumoniae* MOMP and GroEL mRNA levels in host cells infected with live and heat-inactivated (at 60°C for 40 min) *C. pneumoniae.*

3.5 Immunofluorescence and light microscopy of the infected U937 cells

Infected (MOI 4 IFU/cell) and mock-infected U937 cells were harvested 0, 2, 6, 10, 24, and 48 h after infection, and cytospin preparations were made. Cells were fixed with ice-cold acetone and stained with monoclonal mouse anti–*C. pneumoniae* MOMP antibody (Dako). This was followed by an FITC-conjugated anti–mouse secondary antibody (goat $F[ab']_2$ anti–mouse IgG; Sigma). Stained cells were visualized with a confocal laser scanning microscope (model SP II; Leica).

3.6 Human cDNA array production.

Escherichia coli isolates containing plasmids with a cloned insert specific for a particular human gene were obtained from Research Genetics. Inserts were PCR amplified with the universal primers M13 JQ forward (5'-GTTTTCCCAGTCACGACGTTG-3') and M13 JQ reverse (5'-TGAGCGGATAACAATTTCACACAG-3') and were spotted onto a nylon filter by use of the GMS 417 arrayer (Affymetrix). Each array (HA03) contained 2032 individual human genes.

3.7 *U937 RNA amplification, hybridization, and scanning.*

The RNA amplification procedure described elsewhere (Van Gelder, von Zastrow et al. 1990) was followed, with slight modifications. Details of the protocol can be found at http://showelab.wistar.upenn.edu. Labeled targets were prepared from 0.6 μg of amplified RNA (aRNA) with Superscript II reverse transcriptase (Invitrogen), according to the manufacturer's directions, in the presence of 100 μCi of [α-^{33}P] dCTP (Amersham-Pharmacia Biotech), 1 mmol/L dATP, 1 mmol/L dTTP, 1 mmol/L dGTP, 1 μg of oligo-dT (Promega Biosciences), and 1.5 μL of 10× random decamer (Ambion) primers. Labeled cDNA probes were hybridized to individual nylon arrays at 42°C for 18 h. Arrays were washed twice in 2× standard saline citrate (SSC)/1% SDS solution for 20 min at 50°C and were washed once in 0.5× SSC/1% SDS and 0.1× SSC/0.5% SDS for 20 min at 55°C. Arrays were exposed to phosphor screens (Packard Instruments) for 3–5 days and were scanned in a Storm 820 PhosphorImager (Molecular Dynamics). Quantitation of each spot was assessed by ArrayVision image analysis software (Image Research) and was exported to a Microsoft Excel file.

3.8 Data analysis of gene expression.

Normalized signal intensities (nMDs) of individual spots were calculated by subtraction of local background intensity, followed by global normalization and division by the median intensity of all the spots on the array. Statistically significant genes were selected from a data set of 2032 genes, as described below. *Infected versus mock-infected gene expression cutoffs.* A paired *t* test between *C. pneumoniae*– and mock-infected cells was computed for the expression of each gene over all time points for the 3 replicates. In addition, a separate *t* test compared the values at each experimental time point in *C. pneumoniae*–infected cells to the values over all the time points for the mock-infected controls. This comparison allowed detection of transient expression changes in the experimental samples, which were masked by variability in the control experiments. To estimate the number of false-positive findings at a time point, we took the 0-h values to be false positive and estimated the number of true positives detected at 6 h and the later time points by subtracting the 0-h value at $P < .05$. Genes with $P < .05$ in any of the 7 *t* tests described above were considered for further analysis. This gene set was then further reduced by the procedures described below.

Variance cutoff. The variance in the averages over replicates for all time points in infected cells was compared with the analogous variance in mock-infected cells. Only genes with the ratio of variance (average [$nMD_{(inf)}$])/variance average [$nMD_{(mock)}$]) >3 passed this filter, which applied to the set of genes that passed the *t* tests above, selected genes with large changes in the infected cells, compared with mock-infected cells. *Correlation cutoff.* In addition, correlation was obtained between the time course of average gene expression in *C. pneumoniae*–infected cells and the time course in the mock-infected cells. Genes with correlations >0.9 were discarded. This filter eliminated genes that undergo the same changes in both infected and mock-infected cells. *Time course cutoff.* The genes, which passed the three filters described above, were subjected to an additional *t* test comparing the expression values in the *C. pneumoniae*–infected cells only. Depending on the gene expression profile, a *t* test was performed either between the lowest and highest point in the profile or between the continuous set of lowest values and the continuous set of highest values. Genes with $P < .05$ for either of the *t* tests described above passed this filter. This filter selected genes that either increased or decreased significantly from their initial expression value. *Data interpretation.*The significant genes fulfilling all the criteria mentioned above were clustered by using either *k*-means or hierarchical clustering (Eisen, Spellman et al. 1998) analysis based on the *z*-scores of nMDs from mock-infected and/or *C. pneumoniae*–infected cells at each time point, by J-Express software.

3.9 Validation of cDNA array results by real-time PCR..

Either 0.6 μg of aRNA or 1 μg of total RNA from *C. pneumoniae*–infected, heat-inactivated *C. pneumoniae*–infected, mock-infected, and untreated U937 cells harvested at 10, 24, or 48 h after infection were reverse transcribed under the same conditions as in the labeling process. Primer design was based on the determined DNA sequence for the clone spotted on the array by Light Cycler Probe Design Software (version 1.0; Idaho Technology). The primers used are listed in **annex II/** Table 1. Real-time PCR was performed with the LightCycler–FastStart DNA Master SYBR Green I Kit in a Light Cycler instrument (Roche Diagnostics). After 10 min of preincubation at 94°C, 40 cycles were performed with the following conditions: 94°C for 10 s, 55–60°C for 10 s, and 72°C for 20 s. For relative quantitation, a calibration line was generated from the real-time PCR data of

1 : 1, 1 : 10, 1 : 50, or 1 : 100 dilutions of mock-infected U937 cDNA. Duplicates of the 1 : 10 dilution of the tested cDNAs were compared with the calibration line, and the relative amounts of cDNAs were calculated by the Light Cycler analysis 3.01 software. Samples were standardized by using the methyl-CpG binding domain protein 4 gene, which did not change substantially in either the *C. pneumoniae*– or mock-infected U937 cells, as measured by the cDNA arrays.

3.10 Validation of cDNA array results by flow cytometry.

U937 cells were infected with *C. pneumoniae* at a multiplicity of 4 IFU/cell; control cells were mock infected. Infected and mock-infected cells were collected 48 h after infection. Cells were preincubated with normal mouse serum, stained with FITC-labeled mouse anti–human CD44 or CD58 antibody and their appropriate isotype controls (BD Pharmingen), and analyzed within 30 min with an EPICS XL flow cytometer (Beckman-Coulter).

3.11 Chlamydia *strains for epithelial cell line infection and phosphoproteome analysis*

C. trachomatis serovar A strain Har-13, B strain TW-5/OT, Ba strain AP-2/OT, C strain TW-3/OT, D strain UW-3/CX, E strain E/Bour, F strain 1C/Cal-3, G strain UW-524/CX, H strain UW-4/CX, L_1 strain 440/BU, L_2 strain 434/BU, L_3 strain 404/BU, *C. muridarum* strain Nigg, *C. pneumoniae* strain AR-39, and *C. caviae* strain GPIC were propagated in HeLa 229 cells. Infectious EB were purified by density gradient centrifugation, and infection-forming units (IFU) were determined as described previously (Caldwell, Kromhout et al. 1981).

3.12 Chlamydial infection of HeLa 229 and BM12.4 human and mouse epithelial cell lines.

HeLa 229 cells were grown in Dulbecco modified Eagle medium supplemented with 10% fetal bovine serum (DMEM-10) at 37°C in 5% CO_2. Cells were seeded into 24-well tissue culture plates at a density of 5×10^5 cells per ml in DMEM-10, DMEM-10 containing rifampin (1 μg/ml), or emetin (1 μg/ml) and then incubated for 24 h at 37°C.

BM12.4 primary murine oviduct epithelial cells were seeded identically except that they were propagated in 1:1 DMEM-10:F12K (Sigma) medium supplemented with human recombinant FGF-7, as described previously (Johnson 2004). Cell monolayers were incubated on ice for 15 min, washed twice with 4°C Hanks balanced salt solution supplemented with 10 mM HEPES (HBSS), and incubated on ice in 45 μg of DEAE-dextran/ml in HBSS solution for 15 min. After dextran treatment, the EBs suspended in sucrose phosphate glutamic acid buffer were added to the cell layers at various multiplicities of infection (MOI), and the cells were incubated at 4°C for an additional 60 min. To initiate EB entry, the inoculum was aspirated, the cells were washed twice with cold HBSS, and the temperature was shifted to 37°C by adding prewarmed DMEM-0% fetal bovine serum (DMEM-0). After temperature shift (designated time zero in experimental time course infections), the infected and mock-treated cells were incubated at 37°C in 5% CO_2 until protein harvest.

3.13 Western blot detection of chlamydia-induced tyrosine, serine, and threonine phosphorylation in HeLa 229 and BM12.4 cells.

Total cellular proteins from 2 × 10^6 infected HeLa 229 or BM12.4 cells were extracted in 200 μl of 2× Laemmli sample buffer supplemented with 5% (vol/vol) 14.2 M β-mercaptoethanol and denatured at 95°C for 5 min. Proteins were separated on 10% sodium dodecyl sulfate (SDS)-polyacrylamide gels and blotted (100 V, 30 min) onto 0.2-μm-pore-size nitrocellulose membranes (Bio-Rad, Inc.). Membranes were preblocked in TBSTB (1× Tris buffered saline [TBS], 0.1% Tween, 1% bovine serum albumin) solution for 1 h at room temperature. Blots were incubated with primary antiphosphotyrosine antibody 4G10 (1:1,000; Upstate, Lake Placid, N.Y.), antiphosphoserine antibody ab9334-100 (1:200; Abcam, Cambridge, Mass.), or antiphosphothreonine antibody ab9338-50 (1:200; Abcam) in TBSTB overnight at 4°C. Membranes were washed three times (20 min each wash) in TBS supplemented with 0.1% Tween and 5% powdered milk. Washed membranes were incubated with secondary anti-mouse or anti-rabbit horseradish peroxidase-conjugated antibodies for 2 h at room temperature in TBS supplemented with 0.1% Tween and 5% powdered milk and then washed as described above. Proteins were detected by using the

Phototope-HRP Western blot detection system (Cell Signaling Technology, Boston, Mass.) according to the manufacturer's instructions.

3.14 Direct inclusion staining and determination of recoverable IFU.

HeLa 229 monolayers were infected with *C. trachomatis* serovars (B, D, H, and L_2), *C. muridarum* strain mouse pneumonitis (*C.muridarum*), *C. pneumoniae* AR-39, or *C. caviae* strain GPIC, in quadruplicate, at MOI ranging from 0.025 to 1.0, as described above for protein harvest infections and then grown in DMEM-10 at 37°C in 5% CO_2. After inclusion maturation, two wells of each infection condition were methanol fixed at 42 h after infection (*C.muridarum*, *C. caviae* and L_2), 50 h after infection (D, H, and B), and 70 h after infection (*C. pneumoniae*); labeled using primary antichlamydial lipopolysaccharide monoclonal antibody EVI-H1 and secondary fluorescein isothiocyanate-conjugated goat anti-mouse antibody, and photographed at ×100 magnification. To determine recoverable IFU, the two remaining wells from each experimental infection were scraped into 0.5 ml of sucrose phosphate-glutamic acid buffer; the cells were then mechanically disrupted with glass beads, and the lysates were passed onto HeLa 229 monolayers and counted as previously described (Caldwell, Kromhout et al. 1981).

4. Results

4.1 Aim 1. To determine the presence of C. pneumoniae in atherosclerotic and normal human middle cerebral arteries.

4.1.1 C. pneumoniae DNA and C. pneumoniae-like structures could be detected in atherosclerotic but not normal human middle cerebral arteries

The patient characteristics reviewed from the autopsy records and the nPCR results are listed in the **annex I** Table. *C. pneumoniae* DNA was amplified in 5 of the 15 atherosclerotic samples, as demonstrated by a 206-bp DNA fragment visualized by agarose gel electrophoresis, whereas none of the 4 arterial samples from healthy trauma victims were nPCR positive (**annex I**/ Figure 1). Sequencing of nPCR fragments from 2 of the 5 atherosclerotic samples revealed identity to the ompA sequences obtained from the National Center for Biotechnology Information (NCBI) database (http://www.ncbi.nlm.nih.gov). Three of the 5 nPCR-positive cases had symptomatic cerebrovascular disease (cerebral infarct), whereas only 2 of the 10 nPCR-negative cases had symptomatic cerebrovascular disease. The direct cause of death was related to infectious respiratory diseases in 9 of the 15 cases; there was uniform distribution among nPCR-positive and -negative individuals (**annex I**/ Table). TEM of intimal plaques showed structures resembling *C. pneumoniae* elementary bodies in 4 of the 5 nPCR-positive atherosclerotic arterial samples (**annex I**/ Figure 2; Figure 1 in the thesis).

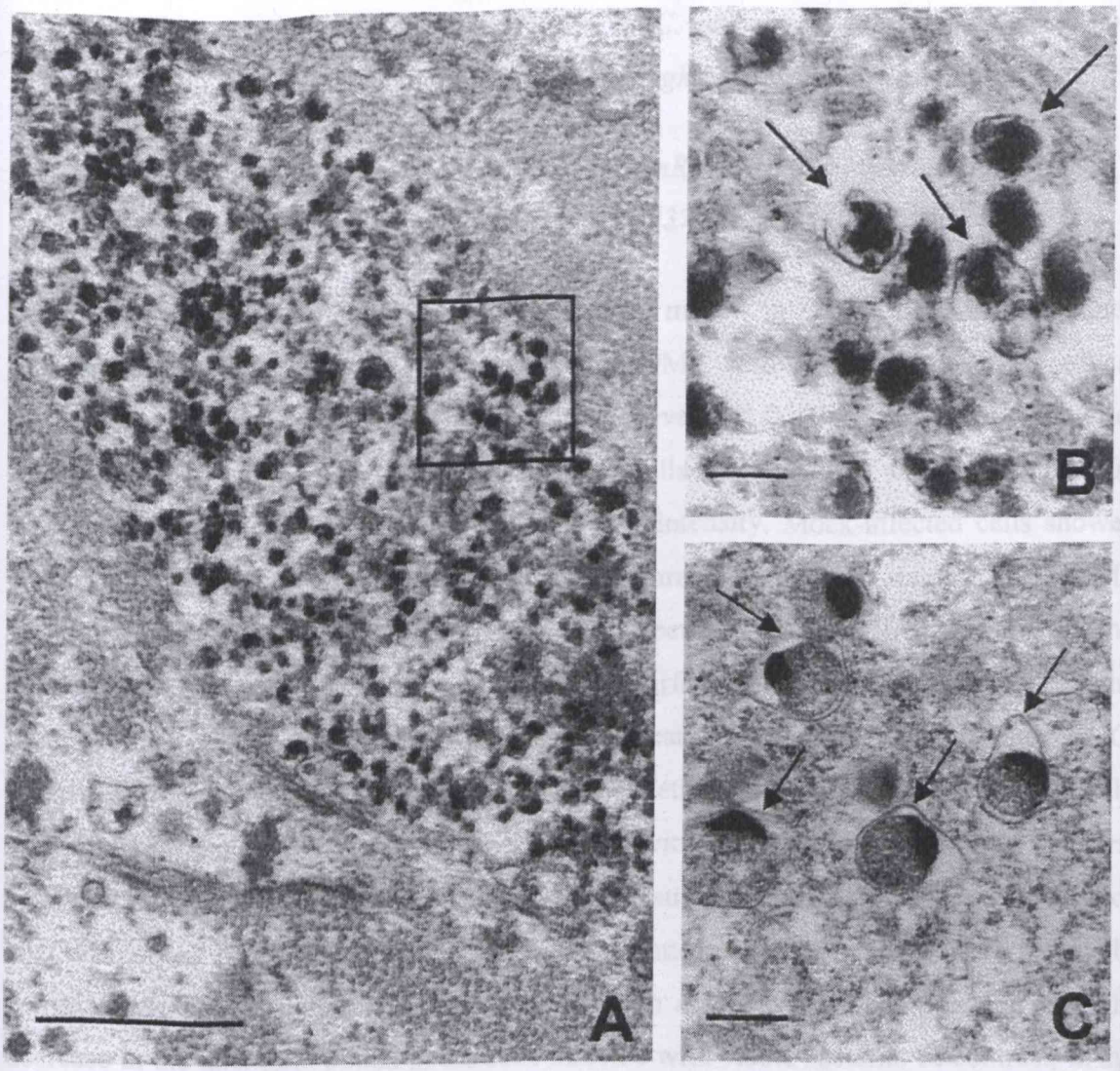

Figure 1. A, TEM of an aggregate of dense bodies in an intimal atheromatous plaque. The very close accumulation of the particles suggests an intracellular localization. The boxed area is shown in panel B. Bar~3.0 μm. B, Pear-shaped structures ~0.3 μm in diameter and similar to *C pneumoniae* elementary bodies (arrows). Bar=0.3 μm. C, *C pneumoniae* elementary bodies (arrows) in a McCoy cell at 48 hours after infection. Bar=0.3 μm.

These structures had a pear-shaped appearance with a dense core (Figures 1A and 1B) and were ~0.3 μm in diameter, ie, similar to the size of the elementary bodies detected in control infected tissue culture cells (Figure 1C). None of the 5 nPCR-negative atherosclerotic samples examined by TEM exhibited *C. pneumoniae*-like structures.

4.2. Aim 2. To obtain a detailed description of C. pneumoniae infection on the gene expression of human monocytes using the high-throughput DNA-chip method.

4.2.1 Detection of C. pneumoniae protein and mRNA in the infected cells shows a maintained viablility of the bacterium in the host U937 cell line.

The presence of *C. pneumoniae* protein and mRNA in U937 cells was determined with monoclonal mouse anti-*C. pneumoniae* MOMP antibody by means of confocal microscopy and quantitative real-time PCR, respectively, at 0, 2, 6, 10, 24, and 48 h after infection. At 0 h after infection, ~70% of the cells were positive for MOMP protein, displaying 1–20 small fluorescing dots of variable intensity. Mock-infected cells showed only dim background fluorescence (**annex II/** Figure 1*D*). Positive staining for MOMP could be detected during the entire course of the experiment (**annex II/** Figure 1*A-C*), and *C. pneumoniae* particles were found both on the surface and inside the cytoplasm of the infected cells (**annex II/** Figure 1*A, insert*), indicating the continuous presence of *C. pneumoniae* in the cells. To further investigate whether *C. pneumoniae* is metabolically active in U937 cells, real-time PCR was performed with 2 different *C. pneumoniae* primers. Expression of MOMP and GroEL genes were measured in host cells infected by live or heat-inactivated *C. pneumoniae*. The expression patterns of the 2 genes were relatively constant, showing a slight increase in transcription at 10 h after infection and a slight decrease in the later time points in the cells infected with viable bacteria. In contrast, in the cells infected with heat-inactivated bacteria, the MOMP and GroEL mRNA levels decreased significantly by 2 h after infection and remained at the same low level during the 48-h time period (**annex II/** Figure 1*E* and 1*F*). The decrease in mRNA levels at the 0 time in the case of MOMP is likely due to degradation of the message pool in the heat-inactivated bacteria during the 45-min centrifugation.

4.2.2 cDNA array analysis shows a significant impact of C. pneumoniae infection on the gene expression of the host U937 cell line.

The transcriptional responses of U937 cells to *C. pneumoniae* and mock infection were examined by cDNA array at 6 time points over a 48-h time course in 3 independent

experiments. The cDNA array contained 2032 unique human genes selected to include functions relating to apoptosis, cell cycle, cell stress, metabolism, signaling, transcription regulation, inflammation, immune response, and cardiovascular disease. To assess the global changes in gene expression as a function of time after infection, we computed 6 *t* tests comparing expression values at individual time points in the *C. pneumoniae*–infected cells with the combined expression values for all time points of the mock-infected cells. The results of these *t* tests are shown in **annex II/** Figure 2. By using the $P < .05$ cutoff and by estimating the number of false positives, as described in Materials and Methods, we detected 67 differentially expressed genes at 6 h, with the numbers increasing to 184 genes at 10 h after infection. Interestingly, this rapid increase in significantly changed genes paralleled the increases in *C. pneumoniae* MOMP and GroEL mRNA expression, which also peaks at 10 h after infection (**annex II/** Figure 1*E* and 1*F*). At 24 and 48 h after infection, the number of differentially expressed genes ($P < .05$) stabilized at ~400 (20%) of all the genes on the array. The seventh curve on the figure, a paired *t* test between all the infected and mock-infected time point data, shows the same number of differentially expressed genes, indicating that the majority of the changes occurred at the later time points. After application of additional filters (see Materials and Methods) to the genes that had a $P < .05$ in any of the 7 *t* tests described above, we find 67 significantly up-regulated genes and 61 significantly down-regulated genes.

4.2.3 Time-course analysis of the significantly up- and down-regulated host genes in response to C. pneumoniae infection reveals nine major gene expression clusters.

When the 128 significant genes were subjected to *k*-means clustering, 6 clusters of up-regulated and 3 clusters of down-regulated genes were obtained (**annex 2/** Figure 3*A* and 3*B*; Figure 2*A* and 2*B* in the thesis).

A

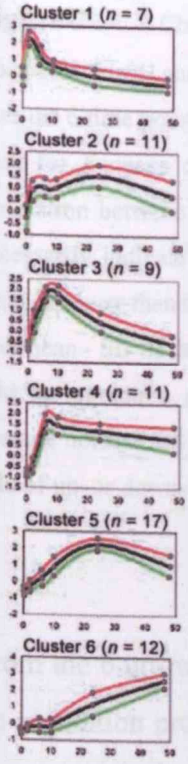

C

Cluster	Gene name	Function	Symbol	Ratio
5	GRO3 oncogene (MIP2B)	Cytokine	GRO3	479.6
2	small inducible cytokine A3 (MIP1A)	Cytokine	SCYA3	291.7
6	pro-platelet basic protein	Cytokine	PPBP	164.8
5	matrix metalloproteinase 10	Tissue remodelling	MMP10	116.1
6	matrix metalloproteinase 3	Tissue remodelling	MMP3	63.0
2	GRO1 oncogene	Cytokine	GRO1	57.4
4	small inducible cytokine A2 (MCP1)	Cytokine	SCYA2	50.3
3	small inducible cytokine A4 (MIP1B)	Cytokine	SCYA4	44.7
5	interleukin 1, beta	Cytokine	IL1B	40.7
6	small inducible cytokine A1, I-309	Cytokine	SCYA1	23.2
6	serpin B7	Tissue remodelling	SERPINB7	17.9
1	NF-kappaB inhibitor alpha	Transcription	NFKBIA	15.4
1	tumor necrosis factor (TNF superfamily, member 2)	Cytokine	TNF	15.4
2	regulator of G-protein signalling 1	Signal transduction	RGS1	11.8
3	tumor necrosis factor, alpha-induced protein 6	CSA*	TNFAIP6	11.6
2	diphtheria toxin receptor (HBEGF)	Cytokine	DTR	11.5
4	Homo sapiens epithelial membrane protein 1 (EMP1)	CSA	EMP1	10.9
5	fatty acid binding protein 4, adipocyte	Cardiovascular	FABP4	10.3
2	ELK3, ETS-domain protein (SRF accessory protein 2)	Transcription	ELK3	10.2
5	plasminogen activator, urokinase	Cardiovascular	PLAU	10.1
5	glycerol kinase	Metabolism	GK	9.4
5	small inducible cytokine A8 (MCP2)	Cytokine	SCYA8	9.2
4	transmembrane protein 2	CSA	TMEM2	7.6
6	matrix metalloproteinase 12 (macrophage elastase)	Tissue remodelling	MMP12	7.3
2	CCAAT/enhancer binding protein (C/EBP), beta	Transcription	CEBPB	7.1
1	tumor necrosis factor, alpha-induced protein 3	Signal transduction	TNFAIP3	7.0
5	Protooncogene SRC, Rous sarcoma	Signal transduction	SRC	5.0
6	CD44 antigen	CSA	CD44	5.0
1	jun B proto-oncogene	Transcription	JUNB	4.7
5	chemokine (C-C motif) receptor 1	CSA	CCR1	4.7
3	tumor necrosis factor (ligand) superfamily, member 7	CSA	TNFSF7	4.3
3	annexin A1	Cardiovascular	ANXA1	4.2
2	coagulation factor V (proaccelerin, labile factor)	Cardiovascular	F5	4.2
4	TRAF family member-associated NFKB activator	Signal transduction	TANK	4.1

B

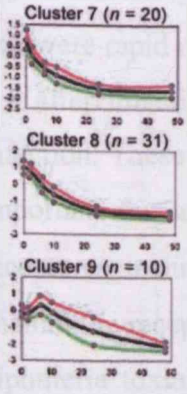

D

Cluster	Gene name	Function	Symbol	Ratio
7	v-myb myeloblastosis viral oncogene homolog (avian)	Transcription	MYB	-26.4
8	MCM7 minichromosome maintenance deficient 7	DNA metabolism	MCM7	-21.2
9	similar to RIKEN cDNA 2610036L13	other	MGC16386	-14.2
7	LIM domain only 2 (rhombotin-like 1)	Cell Cycle	LMO2	-11.2
8	IMP (inosine monophosphate) dehydrogenase 2	Metabolism	IMPDH2	-11.0
7	ribonuclease, RNase A family, 2	RNA metabolism	RNASE2	-10.1
9	kinesin-like 5 (mitotic kinesin-like protein 1)	Cell Cycle	KNSL5	-7.6
7	phosphoribosylaminoimidazole carboxylase	Metabolism	PAICS	-7.2
8	heterogeneous nuclear ribonucleoprotein A1	RNA metabolism	HNRPA1	-7.1
9	cell division cycle 25B	Cell Cycle	CDC25B	-6.5
8	small nuclear ribonucleoprotein D1 polypeptide (16kD)	RNA metabolism	SNRPD1	-6.3
7	matrix Gla protein	other	MGP	-6.0
7	replication factor C (activator 1) 1 (145kD)	DNA metabolism	RFC1	-5.5
7	ligase I, DNA, ATP-dependent	DNA metabolism	LIG1	-5.4
9	kinesin-like 6	Cell Cycle	KNSL6	-4.8
8	heat shock 90kD protein 1, beta	Chaperone	HSPCB	-4.6
7	RAB32, member RAS oncogene family	other	RAB32	-4.6
9	nuclear transport factor 2	Metabolism	NTF2	-4.5
8	sex comb on midleg homolog 1	Transcription	SCMH1	-4.2
9	polo-like kinase (Drosophila)	Cell Cycle	PLK	-4.0
8	interferon consensus sequence binding protein 1	Transcription	ICSBP1	-4.0
8	hypoxanthine phosphoribosyltransferase 1	Metabolism	HPRT1	-3.9
8	protein kinase, DNA-activated, catalytic polypeptide	DNA metabolism	PRKDC	-3.9
7	phosphoribosyl pyrophosphate amidotransferase	Metabolism	PPAT	-3.9
8	nucleophosmin	other	NPM1	-3.8
9	FK506 binding protein 1A (12kD)	Cytoskeleton	FKBP1A	-3.7
7	chromosome 12 open reading frame 8	Metabolism	C12orf8	-3.6
7	serine/arginine repetitive matrix 1	RNA metabolism	SRRM1	-3.6
8	Hs. eukaryotic translation elongation factor 2	Metabolism	EEF2	-3.6
7	Nucleoprotein TPR	Metabolism	TPR	-3.5
8	acetyl-Coenzyme A acetyltransferase 2	Metabolism	ACAT2	-3.5
8	prohibitin	Cell Cycle	PHB	-3.4
9	cyclin-dependent kinase 2	Cell Cycle	CDK2	-3.4
8	mitochondrial ribosomal protein S35	Metabolism	MRPS35	-3.3
9	retinoblastoma binding protein 4	DNA metabolism	RBBP4	-3.2

Figure 2. Changes in gene expression in U937 cells in response to *Chlamydia pneumoniae* infection. Up-regulated *(A)* and down-regulated *(B)* expression profiles of gene clusters in *C. pneumoniae*–infected cells over the 6 time points (0, 2, 6, 10, 24, and 48 h). Gene expression data were normalized, and the *z*-scores were used for *k*-means clustering. *k*-means clustering allocates genes into one of the *k*-clusters according to correlation between the average profile in each cluster and the gene profile. A negative *z*-score does not necessarily indicate that the genes are down-regulated, but rather that the expression at the particular time point is lower than the average expression. The black, red, and green curves represent the mean, mean ± SD, and mean - SD of the *z*-scores of gene expressions related to the particular cluster. Genes that show at least 4-fold up-regulation *(C)* and at least 3-fold down-regulation *(D)*. The ratio reported is calculated with the average normalized signal intensities of the 3 independent experiments at the time point when the maximum fold of up- or down-regulation was measured. CSA, cell surface molecule.

From the 6 up-regulated gene clusters, cluster 1 contained genes with an early and transient up-regulation profile. Important transcriptional regulators—including JunB, NF-κB1, NF-kb inhibitor-α (I-κBα), CCAAT/enhancer binding protein-β (CEBPB), and proinflammatory cytokine tumor necrosis factor (TNF)–α were included among the 7 genes that were rapid responders. Clusters 2 and 4 included genes that were up-regulated early (2–6 h after infection) and then remained at relatively the same level during the course of infection. These clusters contained cell-surface antigens, such as CD82 and CD58, that are important for antigen presentation and the first wave of chemokines and chemokine receptors, including MCP–1, growth-related oncogene (GRO)–1, MIP-1α, and CC chemokine receptor like–2. Other genes with a potential role in atherosclerosis, such as the diphtheria toxin receptor (heparin-binding EGF-like growth factor [HBEGF]), Niemann-Pick disease type C1, and coagulation factor 5, were also found in the clusters. Cluster 3 contained genes that were transiently up-regulated, peaking 6–10 h after infection, including anti-inflammatory genes such as annexin A1 and TNF-α–induced protein 6 (TNFAIP6), a member of the hyaluronan binding family that includes CD44 (Lee, Wisniewski et al. 1992). It is noteworthy that the expression pattern of this gene cluster parallels that of the *C. pneumoniae* MOMP and GroEL genes (**annex II**/ Figure 1*E* and 1*F*). Clusters 5 and 6 contain genes peaking only at 24 and 48 h after infection. These 2 groups include a second wave of up-regulated cytokines and receptors related to chemotaxis, attachment, and

activation, including IL-1β, MCP-2, I-309 (chemokine receptor CCR8 ligand), chemokine receptor–1, G protein–coupled receptor 30, CD44, and integrin-αX. Other genes possibly related to atherosclerosis disease, such as the tissue remodeling genes MMP-3, MMP-10, MMP-12, and proplatelet basic protein (PPBP), the vasoconstrictor endothelin (ET)–1, and lipid metabolism genes, including fatty acid binding protein (FABP)–4 and glycerol kinase, were also in these late responder clusters.

Clusters 7, 8, and 9 contained genes with down-regulated expression levels detected at 2, 6, and 10 h after infection, respectively. The down-regulated gene sets were functionally rather uniform and primarily included genes related to DNA and RNA metabolism, cell-cycle regulation, and growth.

Regarding the fold changes of gene expression in *C. pneumoniae*–infected U937 cells, the most highly up-regulated genes were related to chemotaxis and inflammation. GRO-3 (MIP-2β) exhibited a 480-fold change, small-inducible cytokine A3 (MIP-1α) exhibited a 290-fold change, and PPBP exhibited a 165-fold change. Two tissue-remodeling genes, MMP-10 and MMP-3, were also highly up-regulated (116- and 63-fold, respectively; Figure 2*C*). The most highly down-regulated gene is the proto-oncogene v-myb (26-fold change; Figure 2*D*), which induces proliferation and differentiation of hematopoietic precursors (Karafiat, Dvorakova et al. 2001). The degree to which gene expression was down-regulated was lower in general; only 6 genes were >10-fold down-regulated, compared with the 20 genes that were up-regulated by >10-fold.

To highlight the potential role of *C. pneumoniae* in inflammation and atherosclerosis, a subset of genes with functions related to the innate or acquired immune response and genes associated with atherosclerosis were divided into functional groups and reclustered by means of hierarchical clustering (**annex II**/ Figure 4; Figure 3 in the thesis).

Cardiovascular

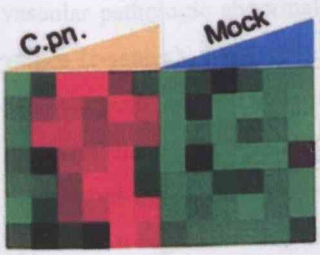

Symbol	Ratio
ANXA1	4.2
F5	4.2
NPC1	1.5
EDN1	3.5
FABP4	10.3
ANXA5	3.0
PLAU	10.1

Tissue remodelling

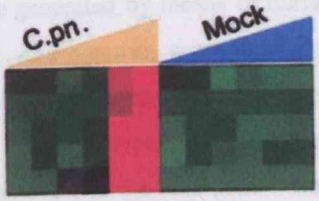

Symbol	Ratio
ADAM9	3.3
MMP3	63.0
SERPINB7	17.9
MMP12	7.3
MMP10	116.1

Cell Surface Antigens

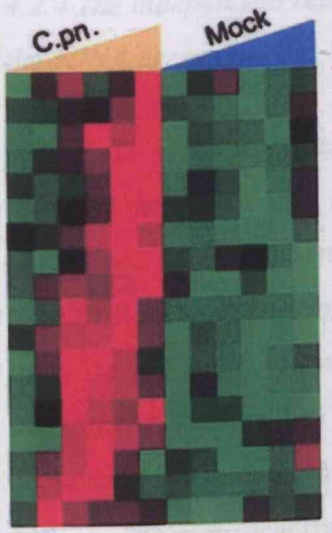

Symbol	Ratio
CD86	2.8
FCGR2B	3.0
KAI1	2.2
CD44	5.0
FCER2	2.2
ITGAX	2.8
GPR30	3.5
CCR1	4.7
CD58	3.4
EMP1	10.9
CCRL2	3.5
TNFAIP6	11.6
TMEM2	7.6
IL4R	2.4
TM4SF1	1.9
TNFSF7	4.3
IFNGR2	2.6
CD83	2.2

Transcription factors

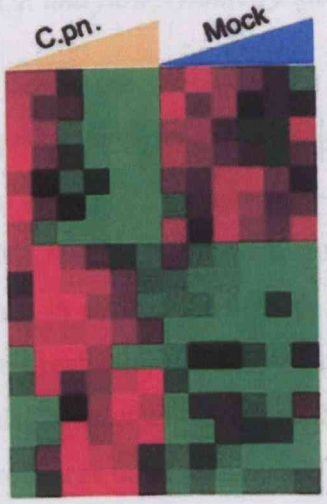

Symbol	Ratio
HDAC2	-2.4
SMARCD2	-2.0
ZNF9	-2.7
ICSBP1	-4.0
TAF5	-2.5
SCMH1	-4.2
MYB	-26.4
JUNB	4.7
NFKBIA	15.4
NFATC1	1.8
ELK3	10.2
NFKB1	2.2
CEBPB	7.1
TFE3	2.8
NCOA1	2.4
CREM	3.8
NR3C1	2.0

Cytokines

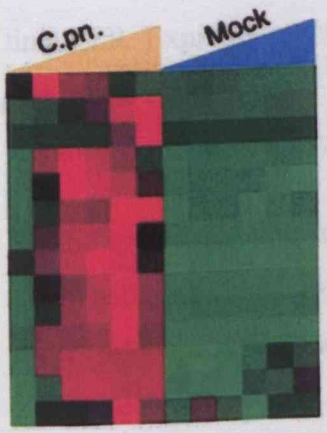

Symbol	Ratio
TNF	15.4
SCYA1	23.2
PPBP	164.8
SCYA4	44.7
SCYA2	50.3
SCYA8	9.2
SCYA3	291.7
DTR	11.5
GRO3	479.6
IL1B	40.7
GRO1	57.4
IL6	2.7
IL1RN	2.9
CSF3	3.5

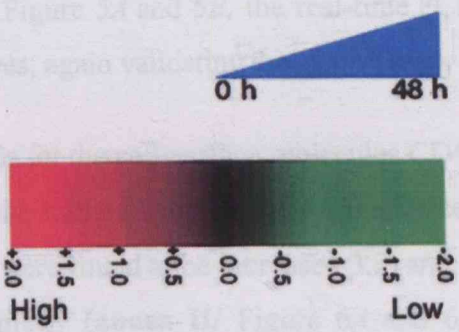

Figure 3. Tree views of differentially expressed genes related to acute and chronic inflammation and vascular pathologic abnormalities. The tree views were generated by means of normalized gene expression values (*z*-scores). Each row represents a single gene. *Red squares,* genes that are overexpressed; *green squares,* genes that are underexpressed, compared with the unchanged expression levels *(black).* The columns represent the 0-, 2-, 6-, 10-, 24-, and 48-h time points. The ratio reported is calculated by using the average normalized signal intensities of the 3 independent experiments at the time point when the maximum fold of up- or down-regulation was measured.

4.2.4 The independent real-time quantitative PCR and flow-cytometry methods confirm the cDNA array data.

To validate the cDNA array data, real-time PCR was performed on 9 genes with different levels of up- and down-regulation in the *C. pneumoniae*–infected cells, as determined by cDNA arrays. By means of cDNA reverse transcribed from aRNA, the real-time PCR results confirmed the cDNA array data in each of the 9 cases and gave a ratio of over- or underexpression either similar to or greater than that determined in the array experiments (**annex II/** Table 2). This was also true when nonamplified RNA was used supporting the linearity of the amplification procedure used (**annex II/** Table 2, columns 2 and 3). The significantly greater levels of change in expression of IL-1β, MMP-10, and PPBP genes detected by PCR could result from nonspecific array cross-hybridization.

The expression profiles of NF-κB1 and its inhibitor, I-κBα, were also assayed by real-time PCR. Expression levels were determined for each time point from the *C. pneumoniae*– and mock-infected cells. As shown in **annex II/** Figure 5*A* and 5*B,* the real-time PCR and cDNA array methods resulted in very similar curves, again validating the cDNA array data.

The array data indicated that the message levels for the cell-surface molecules CD44 and CD58 had a 3.8- and 3.4-fold increase, respectively, in the *C. pneumoniae*–infected cells 48 h after infection. CD44 and CD58 antigen levels were found to be increased 3.2- and 2-fold in the infected cells, as detected by flow cytometry (**annex II/** Figure 6*A* and 6*B*). In addition to confirming the cDNA array results, these data also show that the mRNA and protein levels changed similarly in these 2 cases.

4.3. To determine whether there are differences between the major chlamydial strains during the early interaction of the host cell, particularly comparing the chlamydia-induced early tyrosine-phosphorylation cascade.

4.3.1 C. trachomatis serovar D infection induces rapid, protein synthesis-independent, protein tyrosine phosphorylation in HeLa 229 cells in vitro.

To determine whether the human mucosal pathogen *C. trachomatis* serovar D induces protein tyrosine phosphorylation, HeLa 229 cells were infected at MOI ranging from 0 to 100, and total cellular proteins were harvested 1 h postinfection (p.i.). Extracted proteins were separated by SDS-polyacrylamide gel electrophoresis (PAGE), blotted to nitrocellulose, and probed with the antiphosphotyrosine-specific monoclonal antibody 4G10 (**annex III**/ Fig. 1A). Serovar D infection induced protein tyrosine phosphorylation in HeLa 229 cells in an MOI (multiplicity of infection)-dependent fashion, with the pattern of phosphorylation being most similar to that previously reported for *C. trachomatis* L_2 indicating that the tyrosine phosphorylation induction is a general phenomena of *C. trachomatis* infection. Infection-induced tyrosine-phosphorylated proteins included an intensely labeled complex of proteins migrating with apparent molecular sizes ranging from 70 to 75 kDa (70-kDa complex) induced at MOI of $\geq$ 10, presumably corresponding to the 64- to 68-kDa complex of proteins reported earlier (Birkelund, Johnsen et al. 1994) in association with *C. trachomatis* L_2 infection. A single tyrosine-phosphorylated protein of ~110 kDa, corresponding to the 98-kDa L_2 protein reported earlier (Birkelund, Johnsen et al. 1994), was induced at the same MOI but was less intensely labeled than the 70-kDa complex. Because both the 70-kDa complex and the 110-kDa protein were easily visualized at MOI of 50, this inoculum was used for subsequent kinetic studies. To determine the kinetics of tyrosine phosphorylation, HeLa 229 cells were infected with *C. trachomatis* serovar D at an MOI of 50, and total proteins were harvested at various intervals between 0 and 60 min p.i. Tyrosine phosphorylation of the 70-kDa complex was detectable within 10 min of infection (**annex III**/ Fig. 1B). The labeling intensity increased progressively during the 1-h time course. As previously described for L_2-induced protein

tyrosine phosphorylation (Birkelund, Johnsen et al. 1994), the kinetics, the pattern and intensity of tyrosine-phosphorylated proteins were essentially identical in the presence of host (emetin) or bacterial (rifampin) inhibitors of protein synthesis (**annex III**/ Fig. 1C and D).

4.3.2 Chlamydial induction of protein tyrosine phosphorylation is pathobiotype specific.

Our investigation into phosphorylation induced by *C. trachomatis* serovar D suggested that the pattern of chlamydia-induced protein tyrosine phosphorylation was similar, but not identical, to that previously reported for L_2 (Birkelund, Johnsen et al. 1994). Considering the data in toto, we suspected that phosphorylation might correlate with early infection events that differentiate chlamydial biology in vivo. To test this hypothesis, HeLa 229 cells were infected with *C. trachomatis* trachoma biovars (A, B, Ba, C, D, E, F, G, and H), *C. trachomatis* LGV biovars (L_1, L_2, and L_3), the human respiratory pathogen *C. pneumoniae* AR-39, and the rodent pathogens *C. muridarum* and *C. caviae* GPIC at MOI of 50 and harvested 1 h p.i. Profiles of protein tyrosine phosphorylation induced by chlamydial infection fell into four distinct groups and, surprisingly, these groups sorted the infecting strains into established in vivo pathobiotypes (**annex III**/ Figure 2A; Figure 4A in the thesis). First, the 110-kDa protein (Figure 4B, protein numbered 1) was induced by all *C. trachomatis* strains, including *C.muridarum*. In contrast, neither the more distantly related human pathogen *C. pneumoniae* AR-39 nor *C. caviae* strain GPIC induced phosphorylation of any proteins above background (mock infection) levels (**annex III**/ Figure 2A to C; Figure 4A to C in the thesis). In order to exclude the possibility that the slower growing *C. pneumoniae* AR-39 induces tyrosine phosphorylation later, we extended our tyrosine phosphorylation screen to 2, 4, and 8 h after infection. Both *C. pneumoniae* AR-39 and *C. caviae* GPIC strains failed to induce any detectable tyrosine phosphorylation during this time period (**annex III**/ Figure 2D; Figure 4D in the thesis).

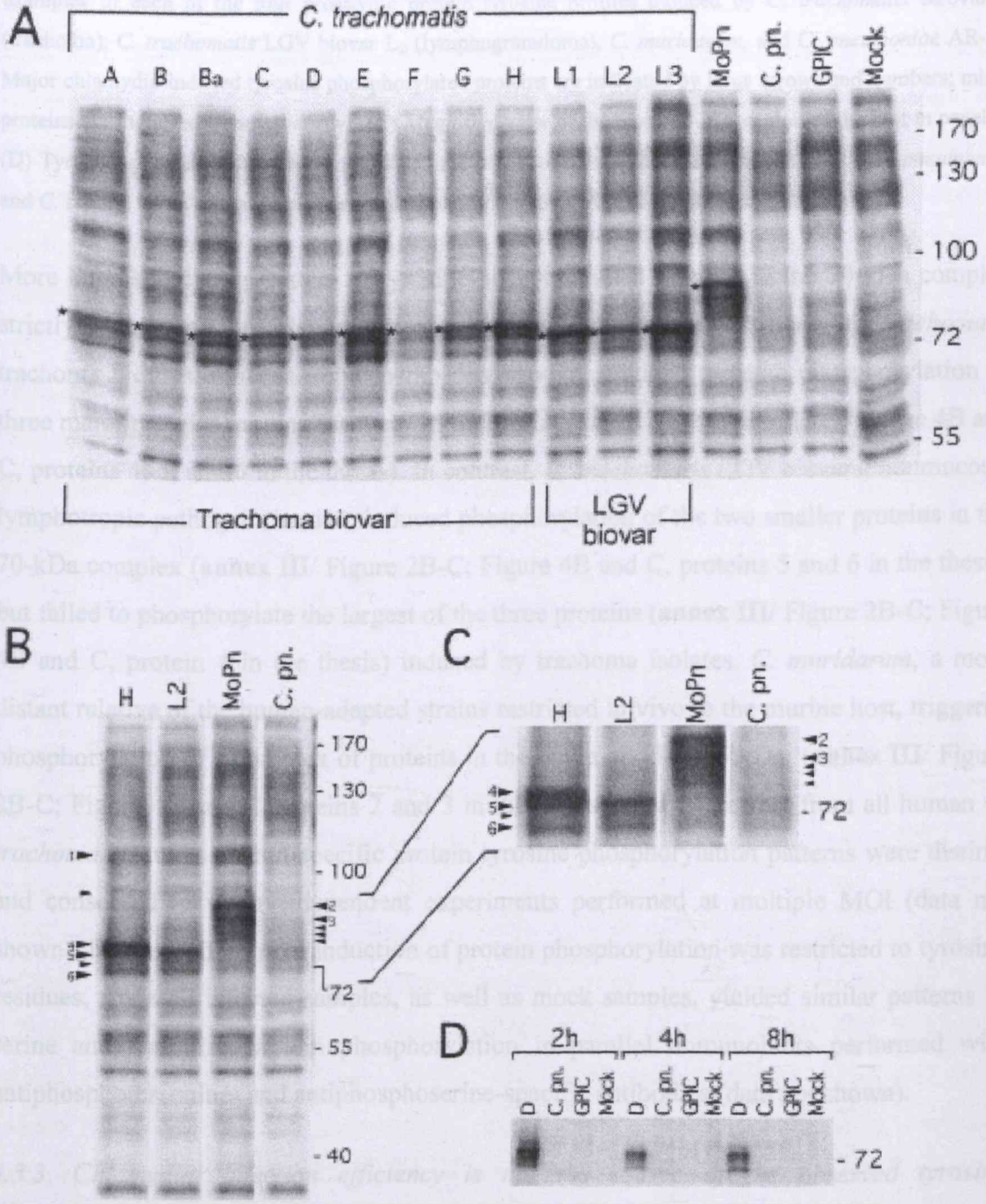

Figure 4. Induction of protein tyrosine phosphorylation by chlamydial infection. (A) HeLa 229 cells were infected with the *C. trachomatis* trachoma biovar serovars (A to H), LGV biovar serovars (L_1, L_2, and L_3), *C. muridarum* strain Nigg (*C.muridarum*), *C. pneumoniae* AR-39, or *C. caviae* GPIC. The most predominant regions of tyrosine phosphorylation are marked with an asterisk. (B) Composite blot from panel A showing

examples of each of the four prototypic protein tyrosine profiles induced by *C. trachomatis* serovar H (trachoma), *C. trachomatis* LGV biovar L_2 (lymphogranuloma), *C. muridarum*, and *C. pneumoniae* AR-39. Major chlamydia-induced tyrosine phosphorylated proteins are indicated by large arrows and numbers; minor proteins are indicated by small arrows. (C) Magnified view of the 65-to 90-kDa region of the blot in panel B. (D) Tyrosine phosphorylation screen at later time points of chlamydial infection shows that *C. pneumoniae* and *C. caviae* GPIC failed to induce tyrosine phosphorylation at 2, 4, and 8 h after infection.

More interestingly, the pattern of tyrosine-phosphorylated proteins in the 70-kDa complex strictly sorted the *C. trachomatis* strains into trachoma and LGV biovars. *C. trachomatis* trachoma biovars, mucosa-tropic pathogens in vivo, induced tyrosine phosphorylation of three major proteins ranging from ca. 75 to 70 kDa (**annex III**/ Figure 2B-C; Figure 4B and C, proteins 4, 5, and 6 in the thesis). In contrast, *C. trachomatis* LGV biovars, nonmucosal lymphotropic pathogens in vivo, induced phosphorylation of the two smaller proteins in the 70-kDa complex (**annex III**/ Figure 2B-C; Figure 4B and C, proteins 5 and 6 in the thesis) but failed to phosphorylate the largest of the three proteins (**annex III**/ Figure 2B-C; Figure 4B and C, protein 4 in the thesis) induced by trachoma isolates. *C. muridarum*, a more distant relative of the human-adapted strains restricted in vivo to the murine host, triggered phosphorylation of a complex of proteins in the range of 75 to 85 kDa (**annex III**/ Figure 2B-C; Figure 4B and C proteins 2 and 3 in the thesis), clearly distinct from all human *C. trachomatis* strains. Strain-specific protein tyrosine phosphorylation patterns were distinct and conserved between independent experiments performed at multiple MOI (data not shown). Further, differential induction of protein phosphorylation was restricted to tyrosine residues, since all infected samples, as well as mock samples, yielded similar patterns of serine and threonine protein phosphorylation in parallel immunoblots performed with antiphosphothreonine- and antiphosphoserine-specific antibodies (data not shown).

4.3.3. Chlamydial infection efficiency is not the source of the observed tyrosine phosphorylation difference in HeLa 229 cells.

Because chlamydial strain-specific patterns of protein tyrosine phosphorylation were repeatable and observed at different MOI in independent experiments, we reasoned that these differences might reflect differential sensitivity of the host HeLa 229 cells to various chlamydial strains. To test this, HeLa 229 cells were infected at different MOI with

the identical chlamydial stocks used in the tyrosine phosphorylation experiments. Infected cells were fixed and chlamydial inclusions visualized by immunofluorescence microscopy (**annex III**/ Figure 3A). In a parallel experiment, inclusions were allowed to mature, and recoverable IFU derived from infections performed at different MOI were determined (**annex III**/ Figure 3B). Both direct inclusion staining and recoverable IFU counts confirmed that essentially equivalent doses of viable chlamydial inoculum were used in determinations of protein tyrosine phosphorylation and that *C. pneumoniae* AR-39 and *C. cavie* GPIC complete their developmental cycles in HeLa 229 host cells. This result strongly argues that the observed differences in phosphorylation profiles reflect fundamental biologic differences between chlamydial strains and that the lack of tyrosine phosphorylation in the case of *C. pneumoniae* and *C. caviae* was not due to the inefficient infection.

4.3.4. Chlamydia strains induce a highly similar tyrosine phosphorylation in human and mouse epithelial cells.

Whether tyrosine-phosphorylated proteins induced by chlamydial infection are of host or bacterial origin remains controversial; data implicating individual *C. trachomatis* serovar L_2-induced tyrosine-phosphorylated proteins deriving from both sources have been reported (Birkelund, Johnsen et al. 1994; Fawaz, van Ooij et al. 1997; Clifton, Fields et al. 2004). In the absence of direct identification of each of these proteins, we reasoned that infection of different host cells might suggest their origin. To test this, we infected HeLa 229 and BM12.4 primary murine oviduct epithelial cells (Johnson 2004) with chlamydial strains at an MOI of 50 and immunoblotted whole-cell lysates harvested 1 h p.i. with 4G10 (**annex III**/ Figure 4). Surprisingly, the infection and strain-specific tyrosine-phosphorylated protein profiles induced by chlamydial infection were nearly identical between the human and mouse cells. In contrast to the conserved infection-induced tyrosine-phosphorylated protein profiles in the three cell lines, the pattern of background 4G10 reactivity differed markedly (**annex III**/ Figure 4). Therefore, the results indicate that the trachoma-induced 70-kDa complex proteins and the *C. muridarum* 75- to 85-kDa complex proteins are of chlamydial origin, however; we cannot exclude the possibility that

four different chlamydia strains induced the phosphorylation of a cohort of conserved host cell proteins with very similar sizes in human and murine cells.

Discussion

5.1 C. pneumoniae has been detected in atherosclerotic tissues at different sites of the vascular system, including the carotid and coronary arteries, the aortic valves, the aorta, and arteries in the lower extremities. A summary of the results from 23 studies indicated that *C. pneumoniae* was detected in 52% (257 of 497) of diseased arteries and in 5% of control vessels by immunohistochemistry or PCR.(Campbell, Kuo et al. 1998) We extended the molecular epidemiology search to the medically important middle cerebral artery region that is frequently related to stroke. We detected the presence of *C. pneumoniae* DNA in 33% of the diseased middle cerebral arterial samples and in none of the controls by nPCR. A review of the autopsy records revealed cerebral infarct in 3 of the 5 nPCR-positive cases, in contrast with only 2 of the 10 nPCR-negative cases. However, the small number of cases did not permit a statistical comparison. A further limitation of the present study is that the detectability of *C. pneumoniae* DNA in the cerebrovascular vessels might be related to age. Because of the younger age of the control individuals and the small numbers of nPCR-positive and -negative cases, statistical comparison is not helpful, and this possibility cannot be excluded. The present study has demonstrated the presence of *C. pneumoniae* DNA in some atherosclerotic samples from middle cerebral arteries, but further studies appear desirable to test for the presence of this organism in these vessels in relation to age and the occurrence of symptomatic cerebrovascular diseases. Because there was no difference in the incidence of respiratory diseases as the direct cause of death among the nPCR-positive and -negative cases, it is improbable that *C. pneumoniae* nPCR positivity was secondary to the infectious diseases, which are rather considered to be terminal-stage diseases that developed a few days before death.

The detection of pear-shaped structures in *C. pneumoniae* nPCR-positive atherosclerotic samples by TEM suggests that not only bacterial DNA but the complete pathogen was also present in the intimal plaque.

A prominent aggregation of dense particles indicates an intracellular accumulation of these structures. The additional presence of this microorganism extracellularly suggests either spontaneous autolysis of the cells followed by bacterial flow into the extracellular matrix or the accumulation of these pathogens outside the cell during a certain stage of their life cycle. *C. pneumoniae* organisms were earlier found by electron microscopy in cells and interstitially in atherosclerotic lesions of the aorta or carotid or coronary arteries, but not in the adjacent nonatherosclerotic tissue.(Taylor-Robinson and Thomas 2000)

The middle cerebral arteries are important sites of cerebral thrombosis. The presence of *C. pneumoniae* in the atheromatous plaques of the middle cerebral artery does not necessarily mean that the organism is a causative agent of the disease; it rather raises the possibility of a role for this bacterium in the pathogenic process. Such a role would point to the value of antibiotic treatment as a means of attenuating cerebrovascular diseases relating to *C. pneumoniae*. Tests on a larger number of cases and age- and sex-matched controls appear warranted, extending to the *C. pneumoniae* serostatus and the presence of *C. pneumoniae* DNA and antigens in vessels other than middle cerebral arteries in the same subjects.

5.2 We have examined the effects of *C. pneumoniae* infection on global gene expression in U937 monocytic cells. Our aim was to determine whether the changes in gene expression that occur support the hypothesis that *C. pneumoniae*–infected monocytes can contribute to the development of atherosclerosis and other diseases associated with inflammation. Other studies that used the same U937 cell line and *C. pneumoniae* AR-39 strain that we used showed that bacterial viability, but probably not replication, can be detected during the initial 48-h time period after infection that we studied (Gaydos, Summersgill et al. 1996; Lin, Campbell et al. 2000; Puolakkainen, Campbell et al. 2003). Our immunofluorescent experiments showed the continuous presence of *C. pneumoniae* inside and on the surface of the U937 cells. In addition, real-time PCR experiments demonstrated that, although bacterial mRNA levels decreased precipitously in cells treated with heat-killed bacteria, mRNA levels were maintained around the steady-state level in cells treated with viable *C. pneumoniae.* It is possible that some of the effects we have recognized are the result of infection, and others are the result of interaction and activation of the host that do not necessarily require the presence of viable bacteria. Although studies

with primary cells will be required to verify our observations in U937 cells, many of the effects on gene expression that we observed in the U937 model were consistent with what is known about monocyte activation.

Our cDNA array results show that infection of U937 cells with *C. pneumoniae* has far-reaching effects on gene transcription within the 48-h time period we have monitored. Significant changes in gene expression were detected in at least 8% of the 1500 expressed genes. Expression levels of 12 of the genes were confirmed either by quantitative real-time PCR or by flow cytometry. In every case, the direction of change detected by the array data was confirmed by our secondary analyses. We detected several classes of genes that were up- or down-regulated soon after infection. For the most part, down-regulated gene expression was detected early and was sustained throughout the 48-h study period. Down-regulated genes were less diverse in function and, in general, were associated with RNA and DNA metabolism, cytoskeleton, cell-cycle regulation, and chromosome maintenance. The most highly down-regulated genes, the Myb oncogene and minichromosome maintenance protein (MCM) 7, are both involved with DNA replication and cell proliferation, Myb at the level of transcription (Karafiat, Dvorakova et al. 2001) and MCM7 at the level of chromosome stability (Labib, Kearsey et al. 2001). The consistent down-regulation of genes related to cell division may be a reflection of the general abatement of cell cycle progression and the associated metabolic pathways. A similar effect was previously observed in the THP1 monocytic cell line after *C. pneumoniae* infection (Yamaguchi, Haranaga et al. 2002).

Genes rapidly up-regulated after infection with *C. pneumoniae* include NF-κB1 and its inhibitor I-κBα, junB, CEBPB, and the important proinflammatory cytokine TNF-α. Expression of each of these early genes has been linked to the induction of the expression of many of the genes associated with inflammation that we find up-regulated at later times, including NF-κB–regulated IL-1, IL-6, TNF-α, MCP-1, MMP-3 (Makarov 2000), junB (AP1 complex)–regulated HBEGF (Park, Adam et al. 1999), MMP-3 (Liacini, Sylvester et al. 2002), and CEBPB-regulated MIP-1α, MIP-1β, granulocyte colony-stimulating factor, and MCP-1 (Ramji and Foka 2002). TNF-α gene expression is both regulated by and can induce NF-κB (Makarov 2000). TNF-α can also induce expression of IL-1, IL-6, plasminogen activator urokinase, MMP, and other molecules, such as TNFAIP6 and

TNFAIP3. Message levels for each of these genes were increased in our infected cultures at later time points. This could be due, in large part, to the effects of TNF-α on NF-κB activation.

Several inflammation-related genes were up-regulated in response to *C. pneumoniae* infection, including chemokines that exhibited high levels of up-regulation (9–480-fold). Expression of these chemokines by monocytes in vivo could trigger the extravasation and local accumulation and activation of neutrophils, monocytes, and lymphocytes. Chemokine expression profiles in the infected cells were similar for the first 24 h after infection. However, although the expression of several chemokines that are chemotactic for neutrophils decreased by 48 h after infection, 2 monocyte-lymphocyte chemokines, I-309 (T cell activator 3) and MCP-2, remained elevated (Figure 3*A*, clusters 5 and 6). It is also noteworthy that, among the 3 chemokine receptors, we found up-regulated expression of CCR1, a receptor for MCP-2, which remained elevated at 48 h (Figure 3*A*, cluster 5). This suggests that a long-term effect of *C. pneumoniae* infection of monocytes could be the expression of chemokines that facilitate mononuclear cell infiltration.

In addition to the induction of inflammation-associated chemokines, *C. pneumoniae* also induced expression of genes for cell-surface molecules that could contribute to the inflammatory process, including CD44, TNFAIP6, and integrin-αX. The expression of CD44 has been shown to contribute to several types of inflammation-related diseases, such as arthritis, experimental encephalomyelitis, colitis, and atherosclerosis (Pure and Cuff 2001). Induction of the hyaluronan receptor CD44 due to *C. pneumoniae* infection has not previously been demonstrated. A second hyaluronan receptor, TNFAIP6, was also highly up-regulated in the present study. The function of TNFAIP6 is less well understood, but its expression has been linked to anti-inflammatory responses (Bardos, Kamath et al. 2001). The expression patterns of these 2 hyaluron receptors were very different. TNFAIP6 expression peaked early and then decreased to baseline level by 48 h after infection (Figure 3*A*, cluster 3). In contrast, the CD44 mRNA levels increased slowly, and, at 48 h after infection, message levels persisted at their highest level (Figure 3*A*, cluster 6). These data suggest that, early in infection, the presence of *C. pneumoniae* can induce not just pro- but also anti-inflammatory genes, as evidenced not only by the expression of TNFAIP6, but also by the expression other anti-inflammatory genes, including annexin A1. This response

appears to be transitory and is eventually superseded by the expression of a variety of proinflammatory chemokines and cytokines and inflammation-associated cell surface markers, including CD44 and integrin-αX.

In general, many of the up-regulated genes were associated with clusters 2 and 5, and particularly 4 and 6, where a majority of the gene expression levels remained at high levels or were still increasing at 48 h. These genes could contribute to a long-term effect on monocytes-macrophage gene expression due to *C. pneumoniae* infection.

A fundamental role for different proinflammatory molecules, such as monocyte chemokines, in the development of chronic inflammatory diseases, such as atherosclerosis or multiple sclerosis, has been described elsewhere (McManus, Berman et al. 1998; Gosling, Slaymaker et al. 1999). The fact that we find chemokines such as MCP-1 to be induced by *C. pneumoniae* supports suggestions that *C. pneumoniae*–infected monocytes may contribute to these inflammatory processes. Continuous tissue remodeling, including local matrix degradation and fibroblast and smooth-muscle cell proliferation, are also characteristic features of atherosclerosis. We also found 3 MMPs—MMP-3, MMP-10, and MMP-12—to be highly up-regulated (63-, 116-, and 7.3-fold, respectively). Additional up-regulated genes include HBEGF and β-thromboglobulin. HBEGF has been shown to induce proliferation of smooth-muscle cells (Higashiyama, Abraham et al. 1991); β-thromboglobulin (part of the up-regulated PPBP) is chemotactic for fibroblasts (Senior, Griffin et al. 1983). HBEGF has also been detected in macrophages in atherosclerotic tissues (Reape, Wilson et al. 1997) and in *C. pneumoniae*–infected endothelial cells (Coombes and Mahony 2001). We also found that important members of the coagulation cascade, coagulation factor V and plasminogen activator urokinase, were up-regulated after *C. pneumoniae* infection, indicating that the local coagulation cascade could also be influenced by *C. pneumoniae*–infected monocytes. Other *C. pneumoniae*–induced genes that could promote atherosclerosis include those involved in either fatty acid or cholesterol trafficking, such as FABP-4 and Niemann-Pick disease type C1. The overexpression of genes responsible for lipid accumulation could be a defensive response of the host cell to infection, because the growth of *C. pneumoniae* is inhibited by high intracellular lipid levels (Blessing, Kuo et al. 2002). However, the lipid accumulation in macrophages also leads to foam-cell formation, which is an early event in the development of atherosclerosis. Finally,

we find that the gene for a highly potent vasoconstrictor, ET-1, is up-regulated (3.5-fold) in infected cells. Induction of ET-1, whose expression has been shown to be important in the pathogenesis of chronic heart disease (Krum, Denver et al. 2001), by *C. pneumoniae* has not been previously demonstrated.

Our findings demonstrate that infection of U937 cells with *C. pneumoniae* rapidly induces gene expression of transcription factors and cell-signaling molecules that then initiate a complex program of gene expression. Many of the large-scale changes in the expression we detected were in genes associated with various steps of acute and chronic inflammation, including leukocyte chemotaxis, attachment, and activation. We also found the induction of a number of genes that could have considerable impact on the initiation and progression of atherosclerosis, including genes associated with lipid accumulation, vasoconstriction, tissue remodeling, and coagulation.

5.3 We could find a pathobiotype specific Tyr-phosphorylation induction in the host epithelial cell, which was clearly different between the *C. trachomatis* mucosal (A-H) and non-mucosal strains (L_1-L_2-L_3) as well as *C. muridarum*, *C. caviae* and *C. pneumoniae*. Using the chlamydial and host cell mRNA and protein synthesis inhibitors rifampicin and emetin, we also showed that this Tyr-phosphorylation uses the already synthesized proteins, and requires a very short period of time, usually ~10 minutes to be induced. This rapid induction suggests, that this phosphorylation is linked to the chlamydial attachment and/or entry. There are at least two possible scenarios exist for the induction of the tyrosine phosphorylation cascade. The first is that the Tyr-phosphorylated proteins have a host origin. In this case there is a chlamydia ligand that clearly distinguishes between the chlamydia pathobiotypes, and somehow the ligand-induced host protein tyrosine phosphorylation also follows this distinction. The chlamydial attachment is a well studied but complex subject, and a number of chlamydial ligands has been implicated in this process including chlamydia hsp70 (Raulston, Davis et al. 2002), omcB (Stephens, Koshiyama et al. 2001) and probably the most widely accepted two: the abundant chlamydia surface molecule major outer membrane protein (MOMP) (Su, Zhang et al. 1988; Su, Raymond et al. 1996), and the heparin and heparane sulphate-GAG on the chlamydial surface (Zhang and Stephens 1992). From the host side, the heparin and heparane sulphate-GAG attached plasma membrane protein was implicated mostly as a

receptor (Byrne 1978; Su, Raymond et al. 1996; Wuppermann, Hegemann et al. 2001). However, there are several indications that these MOMP-GAG or GAG-GAG interactions cannot be the source of the observed Tyr-phosphorylation. Firstly, the surface GAG composition of *C. trachomatis* L_2 and E, and *C. pneumoniae* was found to be remarkably similar (Beswick, Travelstead et al. 2003), but the Tyr-phosphorylation patterns were very different between *C. trachomatis* L_2 and E versus *C. pneumoniae* in our experiments. Moreover, in the same study, heparin treatment of the target bronchial epithelial cells inhibited the infection of *C. pneumoniae* and *C. trachomatis* L_2, but not E, while the Tyr-phosphorylation was similar between L_2 and E and there was no Tyr-phosphorylation induction in the case of *C. pneumoniae* in our study. In an other study, the heparin treatment of HeLa cells strongly (80%) inhibited the attachment of *C. trachomatis* L_2 to the host HeLa cells, but had a various, but generally much lower inhibitory effect on the attachment of *C. trachomatis* serovars B, C and G (2-35%) (Chen and Stephens 1997). The observed differences, that reflect the GAG-GAG interactions between different strains of chlamydia and the host cell does not correlate the Tyr-phosphorylation profile we observed using these serovars. Stephens et al. provided further evidence that the chlamydial GAG – host cell surface interaction is *not* the major source of the observed Tyr-phosphorylation (Stephens, Fawaz et al. 2000). They used heparin coated microbeads to mimic chlamydial attachment and entry, but the beads could only induce a single tyrosine phosphorylated band at the ~80 kD region (*C. muridarum* induction zone), and there was no detectable tyrosine phosphorylation at the ~70 kD region (*C. trachomatis* trachoma and LGV biovars induction zone).

The other frequently cited chlamydial adhesin is the major outer membrane protein, which is a highly expressed, variable surface molecule. The remarkable sequence variation suggests that the molecule has a target of the immune response, and it has been shown before that has an important function as an adhesin (Su, Zhang et al. 1988; Su, Watkins et al. 1990; Su and Caldwell 1991). The MOMP-GAG interaction was showed previously (Su, Raymond et al. 1996): a recombinant MOMP (rMOMP) protein was capable to bind to a heparin and heparane-sulphate component of the host cell surface, and moreover, the rMOMP was able to competitively inhibit the binding of *C. muridarum* to the host HeLa cells. The fact that MOMP has a remarkable variation between the different strains, but this

sequence variation does not distinguish between *C. trachomatis* mucosal and non-mucosal biovars while the observed Tyr-phosphorylation does (Yuan, Zhang et al. 1989; Stothard, Boguslawski et al. 1998), suggests, that this ligand is not involved in Tyr-phosphorylation. We also could not detect an rMOMP induced Tyr-phosphorylation in HeLa cells even when we used various concentrations and timepoints (data not shown). Previous data indicates, that the chlamydial attachment and entry is a complex process involving more than one step. Carabeo et al. isolated a mutant CHO cell line which was capable to bind *C. trachomatis* L_2, but the chlamydia entry was inhibited into these cells, suggesting that the entry is involving more than one step, and possibly more than one chlamydia-host cell ligand-receptor interaction (Carabeo and Hackstadt 2001). If we are applying this model to our results, the chlamydia uses the surface MOMP and/or GAGs to attach the cells as a first "silent" step, and a second ligand to facilitate entry and trigger Tyr-phosphorylation. Among the chlamydial proteins, the polymorphic membrane protein (pmp) gene superfamily has the proper characteristics to be the putative chlamydial ligand, that induces the Tyr-phosphorylation. Some polymorphic membrane proteins are expressed on the EB surface, are targets of neutralizing antibodies, and induce host-cell NF-κB signaling and cytokine secretion (Christiansen, Pedersen et al. 2000; Niessner, Kaun et al. 2003; Stothard, Toth et al. 2003; Wehrl, Brinkmann et al. 2004). Moreover, Stothard et al. (Stothard, Toth et al. 2003) showed substantial variation among pmp genes E, H, and I by restriction fragment length polymorphism analysis of *C. trachomatis* serovars. Of particular relevance to the present study was the finding that such polymorphisms among pmp H correlated exactly with the three major *C. trachomatis* disease groups, prompting Stothard et al. to suggest that the pmp may play a role in pathogenesis (Stothard, Toth et al. 2003). Besides the ligand-receptor interaction that triggers the tyrosine-phosphorylation, the tyrosine phoshphorylated proteins themselves are also unknown. Birkelund et al. labeled the host proteins with S^{35} prior to infection, and immunoprecipitated the tyrosine-phosphorylated proteins after infection. The autofluorography of the precipitated proteins revealed two major bands (97 and 68 kDa) that could be observed in the regular phosphotyrosine specific western blots as well. It indicates that at least partially the tyrosine-phosphorylated proteins have a host cell origin. Based on the fact that the size of the most strongly phosphorylated group of proteins is around 70 kD, Fawaz et al. proposed that this band

could be the 85kD host cell protein cortactin (Fawaz, van Ooij et al. 1997), which has been described previously to be involved in actin cytoskeleton reorganization, a characteristic feature of chlamydial entry into the host cells. They could colocalize the host cortactin to the chlamydial inclusions, in a similar pattern than the observed Tyr-phosphorylation. However when they immunoprecipitated chlamydia infected cell lysates either with anti-cortactin they could not detect an increased phophorylation, indicating that the observed ~70-85 kD protein is not the cortactin.

The second, more simple scenario of the chlamydia induced tyrosine phosphorylation cascade is where there is a chlamydia ligand that differs between the chlamydia pathobiotypes and this protein becomes Tyr-phosphorylated during the attachment and/ or entry. Our observation that strain-specific chlamydia-induced protein tyrosine phosphorylation patterns are common to human and murine host cells supports this hypothesis. Induction of identical, strain-specific protein tyrosine phosphorylation profiles in cells from distant host species argues against the interpretation that these proteins are conserved host proteins of mice and humans. Clifton et al. showed that a high molecular weight chlamydial protein (translocated actin-recruiting phosphoprotein - TARP) that could be involved in the local actin-cytoskeleton reorganization, is secreted into the host cell cytoplasm via a Type III secretion mechanism, and phosphorylated (Clifton, Fields et al. 2004). Type III mediated secretion of chlamydial effectors is a logical and highly favored hypothesis for the delivery of chlamydial effectors to the host cytosol. However, direct evidence for a functional chlamydial type III secretion system is lacking and the most compelling indirect evidence that chlamydiae possess a functional type III apparatus comes from the secretion of putative chlamydial effectors by the Yersina heterologous expression assay (Fields, Mead et al. 2003). The other problem is that the observed size of the phosphorylated chlamydia protein was 150 kD, while in our studies the major phosphorylated bands were around 70kD, and we could not detect a 150 kD band at all. Accordingly, when we used an anti-TARP antibody, one prominent band was detected at the 150 kD region, but no difference at the 70 kD region (data not shown). As a direct consequence of our results, the second scenario also should contain a Tyr-phosphorylation inducing chlamydial ligand that is different between the chlamydia pathobiotypes.

We speculate that the 70-kDa pathobiotype tyrosine-phosphorylated protein(s) may be member(s) of the polymorphic outer membrane protein gene family. The pmp are a polymorphic superfamily of six or more genes, depending on the chlamydial strain, encoding large proteins (90 to 187 kDa) with a distinct homology to type V secreted autotransporters (Grimwood and Stephens 1999; Christiansen, Pedersen et al. 2000; Henderson and Lam 2001; Stothard, Toth et al. 2003). Of interest, pmp genes are absent in the genome of the related parachlamydial symbiont (UWE-25) of free-living amoebae (Horn, Collingro et al. 2004), implying a role for the protein(s) in the infection of mammalian cells. Moreover, as we discussed above, the members of this family are clearly capable to distinguish between the chlamydial pathobiotypes. Intriguingly, the molecular mass of processed pmp is around 70 kDa, a size consistent with that observed for the major tyrosine-phosphorylated protein complex observed during infection with human-adapted *C. trachomatis* strains in this study (Henderson and Lam 2001; Wehrl, Brinkmann et al. 2004). Although the pmp(s) are the most important chlamydial proteins that fulfills the requirements for both tyrosine-phosphorylation scenarios, the role of pmp genes in tyrosine phosphorylation is inconsistent with observations that *C. pneumoniae* and *C. caviae* possess full complements of pmp genes but do not induce tyrosine phosphorylation. One possible explanation is that these pmp genes functionally differ; of the 21 *C. pneumoniae* pmp genes, only two can activate NF-κβ (Niessner, Kaun et al. 2003). *C. trachomatis* and *C. muridarum* may retain a subset of pmp(s) that are stronger inducers of tyrosine phosphorylation. Alternately, *C. pneumoniae* and its genetically close relative, *C. caviae*, might also use unique factors, such as the *Yersinia* YopH protein phosphatase, to mask this signaling event (Bliska, Guan et al. 1991).

The following results are considered novel

- We detected first *C.pneumoniae* DNA, and *C.pneumoniae*-like structures in human middle cerebral artery samples

- We performed the first DNA-chip experiment to study the impact of *C.pneumoniae* on the gene expression of human monocytes discovering several previously not described bacterium induced host genes that can be linked to chlamydia-related chronic infections.

- We described first that the Tyrosine phosphorylation induction is a general phenomenon of *C.trachomatis* infection.

- Our novel finding was, that the induced Tyrosine phosphorylation pattern is clearly different between *C.trachomatis* non-disseminating and disseminating strains.

- We showed first that the various chlamydia strains induced Tyrosine phosphorylation pattern is very similar in human and mouse epithelial cell lines, indicating that the observed Tyrosine phosphorylation have bacterial origin.

6. Acknowledgements

I would like to express my gratitude to key persons shaped my scientific career.

In order of appearance:

Klara Megyeri and Istvan Rosztoczy to introduce me to the basic laboratory work.

Eva Gonczol, my first supervisor, who introduced me into the professional laboratory work, and thought me the fundamental principles of making scientific ideas and performing the follow-up experiments.

Valeria Endresz and Katalin Burian for their helpful discussions, and patience to forgive all the mistakes I made in the lab.

Louise Showe, my first principal investigator in the US, who gave me a detailed training about the principles of high-throughput transcriptome analysis.

Laszlo Kari, for our long discussions about transcriptome analysis and science in general.

Harlan Caldwell, my second principal investigator in the US, who thought me the fine details of scientific hypothesis making, and highlighted many fundamental details of chlamydia research.

Dave Nelson, for our never-ending talks about big ideas in immunology and microbiology.

7. References

Abrams, J. T., B. J. Balin, et al. (2001). "Association between Sezary T cell-activating factor, Chlamydia pneumoniae, and cutaneous T cell lymphoma." Ann N Y Acad Sci **941**: 69-85.

Backert, S., S. Moese, et al. (2001). "Phosphorylation of tyrosine 972 of the Helicobacter pylori CagA protein is essential for induction of a scattering phenotype in gastric epithelial cells." Mol Microbiol **42**(3): 631-44.

Bardos, T., R. V. Kamath, et al. (2001). "Anti-inflammatory and chondroprotective effect of TSG-6 (tumor necrosis factor-alpha-stimulated gene-6) in murine models of experimental arthritis." Am J Pathol **159**(5): 1711-21.

Bea, F., M. H. Puolakkainen, et al. (2003). "Chlamydia pneumoniae induces tissue factor expression in mouse macrophages via activation of Egr-1 and the MEK-ERK1/2 pathway." Circ Res **92**(4): 394-401.

Beswick, E. J., A. Travelstead, et al. (2003). "Comparative studies of glycosaminoglycan involvement in Chlamydia pneumoniae and C. trachomatis invasion of host cells." J Infect Dis **187**(8): 1291-300.

Birkelund, S., H. Johnsen, et al. (1994). "Chlamydia trachomatis serovar L2 induces protein tyrosine phosphorylation during uptake by HeLa cells." Infect Immun **62**(11): 4900-8.

Blessing, E., C. C. Kuo, et al. (2002). "Foam cell formation inhibits growth of Chlamydia pneumoniae but does not attenuate Chlamydia pneumoniae-induced secretion of proinflammatory cytokines." Circulation **105**(16): 1976-82.

Blessing, E., T. M. Lin, et al. (2000). "Chlamydia pneumoniae induces inflammatory changes in the heart and aorta of normocholesterolemic C57BL/6J mice." Infect Immun **68**(8): 4765-8.

Bliska, J. B., K. L. Guan, et al. (1991). "Tyrosine phosphate hydrolysis of host proteins by an essential Yersinia virulence determinant." Proc Natl Acad Sci U S A **88**(4): 1187-91.

Burian, K., K. Berencsi, et al. (2001). "Chlamydia pneumoniae exacerbates aortic inflammatory foci caused by murine cytomegalovirus infection in normocholesterolemic mice." Clin Diagn Lab Immunol **8**(6): 1263-6.

Burian, K., Z. Kis, et al. (2001). "Independent and joint effects of antibodies to human heat-shock protein 60 and Chlamydia pneumoniae infection in the development of coronary atherosclerosis." Circulation **103**(11): 1503-8.

Byrne, G. I. (1978). "Kinetics of phagocytosis of Chlamydia psittaci by mouse fibroblasts (L cells): separation of the attachment and ingestion stages." Infect Immun **19**(2): 607-12.

Caldwell, H. D., J. Kromhout, et al. (1981). "Purification and partial characterization of the major outer membrane protein of Chlamydia trachomatis." Infect Immun **31**(3): 1161-76.

Campbell, L. A., C. C. Kuo, et al. (1998). "Chlamydia pneumoniae and cardiovascular disease." Emerg Infect Dis **4**(4): 571-9.

Campbell, L. A., M. Rosenfeld, et al. (2000). "The role of Chlamydia pneumoniae in atherosclerosis--recent evidence from animal models." Trends Microbiol **8**(6): 255-7; discussion 257.

Carabeo, R. A., S. S. Grieshaber, et al. (2002). "Chlamydia trachomatis induces remodeling of the actin cytoskeleton during attachment and entry into HeLa cells." Infect Immun **70**(7): 3793-803.

Carabeo, R. A. and T. Hackstadt (2001). "Isolation and characterization of a mutant Chinese hamster ovary cell line that is resistant to Chlamydia trachomatis infection at a novel step in the attachment process." Infect Immun **69**(9): 5899-904.

Chen, J. C. and R. S. Stephens (1997). "Chlamydia trachomatis glycosaminoglycan-dependent and independent attachment to eukaryotic cells." Microb Pathog **22**(1): 23-30.

Christiansen, G., A. S. Pedersen, et al. (2000). "Potential relevance of Chlamydia pneumoniae surface proteins to an effective vaccine." J Infect Dis **181 Suppl 3**: S528-37.

Clifton, D. R., K. A. Fields, et al. (2004). "A chlamydial type III translocated protein is tyrosine-phosphorylated at the site of entry and associated with recruitment of actin." Proc Natl Acad Sci U S A **101**(27): 10166-71.

Clifton, D. R., K. A. Fields, et al. (2004). "A chlamydial type III translocated protein is tyrosine-phosphorylated at the site of entry and associated with recruitment of actin." Proc Natl Acad Sci U S A.

Cook, P. J., D. Honeybourne, et al. (1998). "Chlamydia pneumoniae antibody titers are significantly associated with acute stroke and transient cerebral ischemia: the West Birmingham Stroke Project." Stroke **29**(2): 404-10.

Coombes, B. K. and J. B. Mahony (2001). "cDNA array analysis of altered gene expression in human endothelial cells in response to Chlamydia pneumoniae infection." Infect Immun **69**(3): 1420-7.

Eisen, M. B., P. T. Spellman, et al. (1998). "Cluster analysis and display of genome-wide expression patterns." Proc Natl Acad Sci U S A **95**(25): 14863-8.

Elkind, M. S., I. F. Lin, et al. (2000). "Chlamydia pneumoniae and the risk of first ischemic stroke: The Northern Manhattan Stroke Study." Stroke **31**(7): 1521-5.

Esposito, S. and N. Principi (2001). "Asthma in children: are chlamydia or mycoplasma involved?" Paediatr Drugs **3**(3): 159-68.

Fagerberg, B., J. Gnarpe, et al. (1999). "Chlamydia pneumoniae but not cytomegalovirus antibodies are associated with future risk of stroke and cardiovascular disease: a prospective study in middle-aged to elderly men with treated hypertension." Stroke **30**(2): 299-305.

Fawaz, F. S., C. van Ooij, et al. (1997). "Infection with Chlamydia trachomatis alters the tyrosine phosphorylation and/or localization of several host cell proteins including cortactin." Infect Immun **65**(12): 5301-8.

Fields, K. A., D. J. Mead, et al. (2003). "Chlamydia trachomatis type III secretion: evidence for a functional apparatus during early-cycle development." Mol Microbiol **48**(3): 671-83.

Fredricks, D. N. and D. A. Relman (1999). "Application of polymerase chain reaction to the diagnosis of infectious diseases." Clin Infect Dis **29**(3): 475-86; quiz 487-8.

Gaydos, C. A., J. T. Summersgill, et al. (1996). "Replication of Chlamydia pneumoniae in vitro in human macrophages, endothelial cells, and aortic artery smooth muscle cells." Infect Immun **64**(5): 1614-20.

Gilbert A, L. G. "Arterites infectieuses experimentales." Comptes Rendus Hebdomadaires des Seances et Memoires de la Societe de Biologie **41**: 583-4.

Gosling, J., S. Slaymaker, et al. (1999). "MCP-1 deficiency reduces susceptibility to atherosclerosis in mice that overexpress human apolipoprotein B." J Clin Invest **103**(6): 773-8.

Grayston, J. T. (2000). "Background and current knowledge of Chlamydia pneumoniae and atherosclerosis." J Infect Dis **181 Suppl 3**: S402-10.

Grimwood, J. and R. S. Stephens (1999). "Computational analysis of the polymorphic membrane protein superfamily of Chlamydia trachomatis and Chlamydia pneumoniae." Microb Comp Genomics **4**(3): 187-201.

Hawrani, A., C. E. Dempsey, et al. (2003). "Effect of protein kinase A-mediated phosphorylation on the structure and association properties of the enteropathogenic Escherichia coli Tir virulence protein." J Biol Chem **278**(28): 25839-46.

Henderson, I. R. and A. C. Lam (2001). "Polymorphic proteins of Chlamydia spp.--autotransporters beyond the Proteobacteria." Trends Microbiol **9**(12): 573-8.

Higashiyama, S., J. A. Abraham, et al. (1991). "A heparin-binding growth factor secreted by macrophage-like cells that is related to EGF." Science **251**(4996): 936-9.

Higgins, J. P. (2003). "Chlamydia pneumoniae and coronary artery disease: the antibiotic trials." Mayo Clin Proc **78**(3): 321-32.

Horn, M., A. Collingro, et al. (2004). "Illuminating the evolutionary history of chlamydiae." Science **304**(5671): 728-30.

Johnson, R. M. (2004). "Murine oviduct epithelial cell cytokine responses to Chlamydia muridarum infection include interleukin-12-p70 secretion." Infect Immun **72**(7): 3951-60.

Kalayoglu, M. V. and G. I. Byrne (1998). "Induction of macrophage foam cell formation by Chlamydia pneumoniae." J Infect Dis **177**(3): 725-9.

Kalman, S., W. Mitchell, et al. (1999). "Comparative genomes of Chlamydia pneumoniae and C. trachomatis." Nat Genet **21**(4): 385-9.

Karafiat, V., M. Dvorakova, et al. (2001). "The leucine zipper region of Myb oncoprotein regulates the commitment of hematopoietic progenitors." Blood **98**(13): 3668-76.

Kaul, R. and W. M. Wenman (2001). "Chlamydia pneumoniae facilitates monocyte adhesion to endothelial and smooth muscle cells." Microb Pathog **30**(3): 149-55.

Kenny, B., R. DeVinney, et al. (1997). "Enteropathogenic E. coli (EPEC) transfers its receptor for intimate adherence into mammalian cells." Cell **91**(4): 511-20.

Kim, M. P., C. A. Gaydos, et al. (2005). "Chlamydia pneumoniae enhances cytokine-stimulated human monocyte matrix metalloproteinases through a prostaglandin E2-dependent mechanism." Infect Immun **73**(1): 632-4.

Kothe, H., K. Dalhoff, et al. (2000). "Hydroxymethylglutaryl coenzyme A reductase inhibitors modify the inflammatory response of human macrophages and endothelial cells infected with Chlamydia pneumoniae." Circulation **101**(15): 1760-3.

Krum, H., R. Denver, et al. (2001). "Diagnostic and therapeutic potential of the endothelin system in patients with chronic heart failure." Heart Fail Rev **6**(4): 341-52.

Kuo, C. C. and J. T. Grayston (1990). "A sensitive cell line, HL cells, for isolation and propagation of Chlamydia pneumoniae strain TWAR." J Infect Dis **162**(3): 755-8.

Labib, K., S. E. Kearsey, et al. (2001). "MCM2-7 proteins are essential components of prereplicative complexes that accumulate cooperatively in the nucleus during G1-phase and are required to establish, but not maintain, the S-phase checkpoint." Mol Biol Cell **12**(11): 3658-67.

Lee, T. H., H. G. Wisniewski, et al. (1992). "A novel secretory tumor necrosis factor-inducible protein (TSG-6) is a member of the family of hyaluronate binding proteins, closely related to the adhesion receptor CD44." J Cell Biol **116**(2): 545-57.

Liacini, A., J. Sylvester, et al. (2002). "Inhibition of interleukin-1-stimulated MAP kinases, activating protein-1 (AP-1) and nuclear factor kappa B (NF-kappa B) transcription factors down-regulates matrix metalloproteinase gene expression in articular chondrocytes." Matrix Biol **21**(3): 251-62.

Libby, P. (2002). "Inflammation in atherosclerosis." Nature **420**(6917): 868-74.

Lin, T. M., L. A. Campbell, et al. (2000). "Monocyte-endothelial cell coculture enhances infection of endothelial cells with Chlamydia pneumoniae." J Infect Dis **181**(3): 1096-100.

Makarov, S. S. (2000). "NF-kappaB as a therapeutic target in chronic inflammation: recent advances." Mol Med Today **6**(11): 441-8.

May, A. E., V. Redecke, et al. (2003). "Recruitment of Chlamydia pneumoniae-infected macrophages to the carotid artery wall in noninfected, nonatherosclerotic mice." Arterioscler Thromb Vasc Biol **23**(5): 789-94.

McManus, C., J. W. Berman, et al. (1998). "MCP-1, MCP-2 and MCP-3 expression in multiple sclerosis lesions: an immunohistochemical and in situ hybridization study." J Neuroimmunol **86**(1): 20-9.

Moazed, T. C., L. A. Campbell, et al. (1999). "Chlamydia pneumoniae infection accelerates the progression of atherosclerosis in apolipoprotein E-deficient mice." J Infect Dis **180**(1): 238-41.

Moazed, T. C., C. Kuo, et al. (1997). "Murine models of Chlamydia pneumoniae infection and atherosclerosis." J Infect Dis **175**(4): 883-90.

Moazed, T. C., C. Kuo, et al. (1996). "Experimental rabbit models of Chlamydia pneumoniae infection." Am J Pathol **148**(2): 667-76.

Moazed, T. C., C. C. Kuo, et al. (1998). "Evidence of systemic dissemination of Chlamydia pneumoniae via macrophages in the mouse." J Infect Dis **177**(5): 1322-5.

Netea, M. G., B. J. Kullberg, et al. (2002). "Non-LPS components of Chlamydia pneumoniae stimulate cytokine production through Toll-like receptor 2-dependent pathways." Eur J Immunol **32**(4): 1188-95.

Netea, M. G., C. H. Selzman, et al. (2000). "Acellular components of Chlamydia pneumoniae stimulate cytokine production in human blood mononuclear cells." Eur J Immunol **30**(2): 541-9.

Niessner, A., C. Kaun, et al. (2003). "Polymorphic membrane protein (PMP) 20 and PMP 21 of Chlamydia pneumoniae induce proinflammatory mediators in human endothelial cells in vitro by activation of the nuclear factor-kappaB pathway." J Infect Dis **188**(1): 108-13.

Pace, J., M. J. Hayman, et al. (1993). "Signal transduction and invasion of epithelial cells by S. typhimurium." Cell **72**(4): 505-14.

Park, J. M., R. M. Adam, et al. (1999). "AP-1 mediates stretch-induced expression of HB-EGF in bladder smooth muscle cells." Am J Physiol **277**(2 Pt 1): C294-301.

Pfaller, M. A. (2001). "Molecular approaches to diagnosing and managing infectious diseases: practicality and costs." Emerg Infect Dis **7**(2): 312-8.

Puolakkainen, M., L. A. Campbell, et al. (2003). "Cell-to-cell contact of human monocytes with infected arterial smooth-muscle cells enhances growth of Chlamydia pneumoniae." J Infect Dis **187**(3): 435-40.

Puolakkainen, M., C. C. Kuo, et al. (2005). "Chlamydia pneumoniae uses the mannose 6-phosphate/insulin-like growth factor 2 receptor for infection of endothelial cells." Infect Immun **73**(8): 4620-5.

Pure, E. and C. A. Cuff (2001). "A crucial role for CD44 in inflammation." Trends Mol Med **7**(5): 213-21.

Ramji, D. P. and P. Foka (2002). "CCAAT/enhancer-binding proteins: structure, function and regulation." Biochem J **365**(Pt 3): 561-75.

Raulston, J. E., C. H. Davis, et al. (2002). "Surface accessibility of the 70-kilodalton Chlamydia trachomatis heat shock protein following reduction of outer membrane protein disulfide bonds." Infect Immun **70**(2): 535-43.

Reape, T. J., V. J. Wilson, et al. (1997). "Detection and cellular localization of heparin-binding epidermal growth factor-like growth factor mRNA and protein in human atherosclerotic tissue." J Mol Cell Cardiol **29**(6): 1639-48.

Rosenshine, I., M. S. Donnenberg, et al. (1992). "Signal transduction between enteropathogenic Escherichia coli (EPEC) and epithelial cells: EPEC induces

tyrosine phosphorylation of host cell proteins to initiate cytoskeletal rearrangement and bacterial uptake." Embo J **11**(10): 3551-60.

Saikku, P., M. Leinonen, et al. (1988). "Serological evidence of an association of a novel Chlamydia, TWAR, with chronic coronary heart disease and acute myocardial infarction." Lancet **2**(8618): 983-6.

Sander, D., K. Winbeck, et al. (2002). "Reduced progression of early carotid atherosclerosis after antibiotic treatment and Chlamydia pneumoniae seropositivity." Circulation **106**(19): 2428-33.

Sander, D., K. Winbeck, et al. (2004). "Progression of early carotid atherosclerosis is only temporarily reduced after antibiotic treatment of Chlamydia pneumoniae seropositivity." Circulation **109**(8): 1010-5.

Segal, E. D., J. Cha, et al. (1999). "Altered states: involvement of phosphorylated CagA in the induction of host cellular growth changes by Helicobacter pylori." Proc Natl Acad Sci U S A **96**(25): 14559-64.

Segal, E. D., S. Falkow, et al. (1996). "Helicobacter pylori attachment to gastric cells induces cytoskeletal rearrangements and tyrosine phosphorylation of host cell proteins." Proc Natl Acad Sci U S A **93**(3): 1259-64.

Senior, R. M., G. L. Griffin, et al. (1983). "Chemotactic activity of platelet alpha granule proteins for fibroblasts." J Cell Biol **96**(2): 382-5.

Stephens, R. S., F. S. Fawaz, et al. (2000). "Eukaryotic cell uptake of heparin-coated microspheres: a model of host cell invasion by Chlamydia trachomatis." Infect Immun **68**(3): 1080-5.

Stephens, R. S., K. Koshiyama, et al. (2001). "Heparin-binding outer membrane protein of chlamydiae." Mol Microbiol **40**(3): 691-9.

Stothard, D. R., G. Boguslawski, et al. (1998). "Phylogenetic analysis of the Chlamydia trachomatis major outer membrane protein and examination of potential pathogenic determinants." Infect Immun **66**(8): 3618-25.

Stothard, D. R., G. A. Toth, et al. (2003). "Polymorphic membrane protein H has evolved in parallel with the three disease-causing groups of Chlamydia trachomatis." Infect Immun **71**(3): 1200-8.

Su, H. and H. D. Caldwell (1991). "In vitro neutralization of Chlamydia trachomatis by monovalent Fab antibody specific to the major outer membrane protein." Infect Immun **59**(8): 2843-5.

Su, H., L. Raymond, et al. (1996). "A recombinant Chlamydia trachomatis major outer membrane protein binds to heparan sulfate receptors on epithelial cells." Proc Natl Acad Sci U S A **93**(20): 11143-8.

Su, H., N. G. Watkins, et al. (1990). "Chlamydia trachomatis-host cell interactions: role of the chlamydial major outer membrane protein as an adhesin." Infect Immun **58**(4): 1017-25.

Su, H., Y. X. Zhang, et al. (1988). "Differential effect of trypsin on infectivity of Chlamydia trachomatis: loss of infectivity requires cleavage of major outer membrane protein variable domains II and IV." Infect Immun **56**(8): 2094-100.

Subtil, A., B. Wyplosz, et al. (2004). "Analysis of Chlamydia caviae entry sites and involvement of Cdc42 and Rac activity." J Cell Sci **117**(Pt 17): 3923-33.

Taylor-Robinson, D. and B. J. Thomas (2000). "Chlamydia pneumoniae in atherosclerotic tissue." J Infect Dis **181 Suppl 3**: S437-40.

Thylefors, B., A. D. Negrel, R. Pararajasegaram, K. Y. Dadzie (1995). Global data on blindness.

Tong, C. Y. and M. Sillis (1993). "Detection of Chlamydia pneumoniae and Chlamydia psittaci in sputum samples by PCR." J Clin Pathol **46**(4): 313-7.

Van Gelder, R. N., M. E. von Zastrow, et al. (1990). "Amplified RNA synthesized from limited quantities of heterogeneous cDNA." Proc Natl Acad Sci U S A **87**(5): 1663-7.

Vehmaan-Kreula, P., M. Puolakkainen, et al. (2001). "Chlamydia pneumoniae proteins induce secretion of the 92-kDa gelatinase by human monocyte- derived macrophages." Arterioscler Thromb Vasc Biol **21**(1): E1-8.

Vink, A., M. Poppen, et al. (2001). "Distribution of Chlamydia pneumoniae in the human arterial system and its relation to the local amount of atherosclerosis within the individual." Circulation **103**(12): 1613-7.

Virok, D., Z. Kis, et al. (2006). "Chlamydophila pneumoniae and human cytomegalovirus in atherosclerotic carotid plaques--combined presence and possible interactions." Acta Microbiol Immunol Hung **53**(1): 35-50.

Wehrl, W., V. Brinkmann, et al. (2004). "From the inside out--processing of the Chlamydial autotransporter PmpD and its role in bacterial adhesion and activation of human host cells." Mol Microbiol **51**(2): 319-34.

WHO (1996). Global prevalence and incidence of selected curable sexually transmitted diseases: overview and estimates. Geneva, Switzerland.

Wimmer, M. L., R. Sandmann-Strupp, et al. (1996). "Association of chlamydial infection with cerebrovascular disease." Stroke **27**(12): 2207-10.

Wuppermann, F. N., J. H. Hegemann, et al. (2001). "Heparan sulfate-like glycosaminoglycan is a cellular receptor for Chlamydia pneumoniae." J Infect Dis **184**(2): 181-7.

Yamaguchi, H., S. Haranaga, et al. (2002). "Chlamydia pneumoniae infection induces differentiation of monocytes into macrophages." Infect Immun **70**(5): 2392-8.

Yuan, Y., Y. X. Zhang, et al. (1989). "Nucleotide and deduced amino acid sequences for the four variable domains of the major outer membrane proteins of the 15 Chlamydia trachomatis serovars." Infect Immun **57**(4): 1040-9.

Yucesan, C. and S. Sriram (2001). "Chlamydia pneumoniae infection of the central nervous system." Curr Opin Neurol **14**(3): 355-9.

Zhang, J. P. and R. S. Stephens (1992). "Mechanism of C. trachomatis attachment to eukaryotic host cells." Cell **69**(5): 861-9.

8. Annex

Annex I.